Scaling up irrigation for food-system resilience under abrupt sunlight reduction: A global optimisation analysis

Pinkeshkumar Attarwala[1,2,*], Simon Blouin[1,], Mike Hinge[1], Luisa Lopes Monteiro[1,2,], Mohammadreza Ebrahimnataj Tiji[1,2,], Thomas Cochrane[3], David Denkenberger[1,2,]
[1]Alliance to Feed the Earth in Disasters (ALLFED) Lafayette, CO 80026, USA;
[2]Department of Mechanical Engineering, University of Canterbury, Private Bag 4800 Christchurch 8140, New Zealand;
[3]Department of Civil and Environmental Engineering, University of Canterbury, Private Bag 4800 Christchurch 8140, New Zealand;
[*]Correspondence: pinkeshkumar.attarwala@pg.canterbury.ac.nz;

Abstract

Abrupt sunlight-reduction scenarios (ASRSs), such as nuclear winter or massive volcanic eruptions, could suppress temperatures and incoming solar radiation for several years, sharply reducing agricultural productivity and creating a severe threat of global food insecurity. Prior literature indicates that expanding cultivated area can offset a portion of these yield losses, but no estimates exist for the contribution of new and scaled-up irrigation infrastructure to food security under ASRS conditions, whether on existing croplands or on lands suitable for expansion. We quantify the food-security benefit of groundwater-based irrigation investment under a 150-Tg soot scenario using a global 1° gridded framework, with yields and water requirements for six key staple crops drawn from crop simulation models. We assess irrigation investment opportunities on both existing rainfed croplands and suitable expansion areas, allocating budgets sequentially to maximise the marginal caloric return per unit of investment. Early, low-cost gains along the supply curve are dominated by rainfed production on existing cropland and continued legacy irrigation, with new pivot irrigation entering mainly at higher budgets. Expanding cultivation onto herbaceous, shrub, barren, and young-forest land tends to be more expensive per calorie produced, yet becomes increasingly important once lower-cost opportunities are exhausted. At the $8.935 trillion budget, total modelled production is equivalent to feeding about 10.4 billion people per year; of that, the yield gain from new and upgraded irrigation relative to rainfed production on the same parcels is about 2.8 billion people per year, and produces as much grain as today. Assuming labor and input prices remain unchanged, the marginal cost of matching global staple production at current levels on average under ASRS reaches approximately $611 per tonne of dry carbohydrate equivalent, against typical wheat prices of $240–290 per tonne of dry carbohydrate equivalent.

Keywords: nuclear winter, irrigation, global catastrophic risk, crop modelling, resilient foods

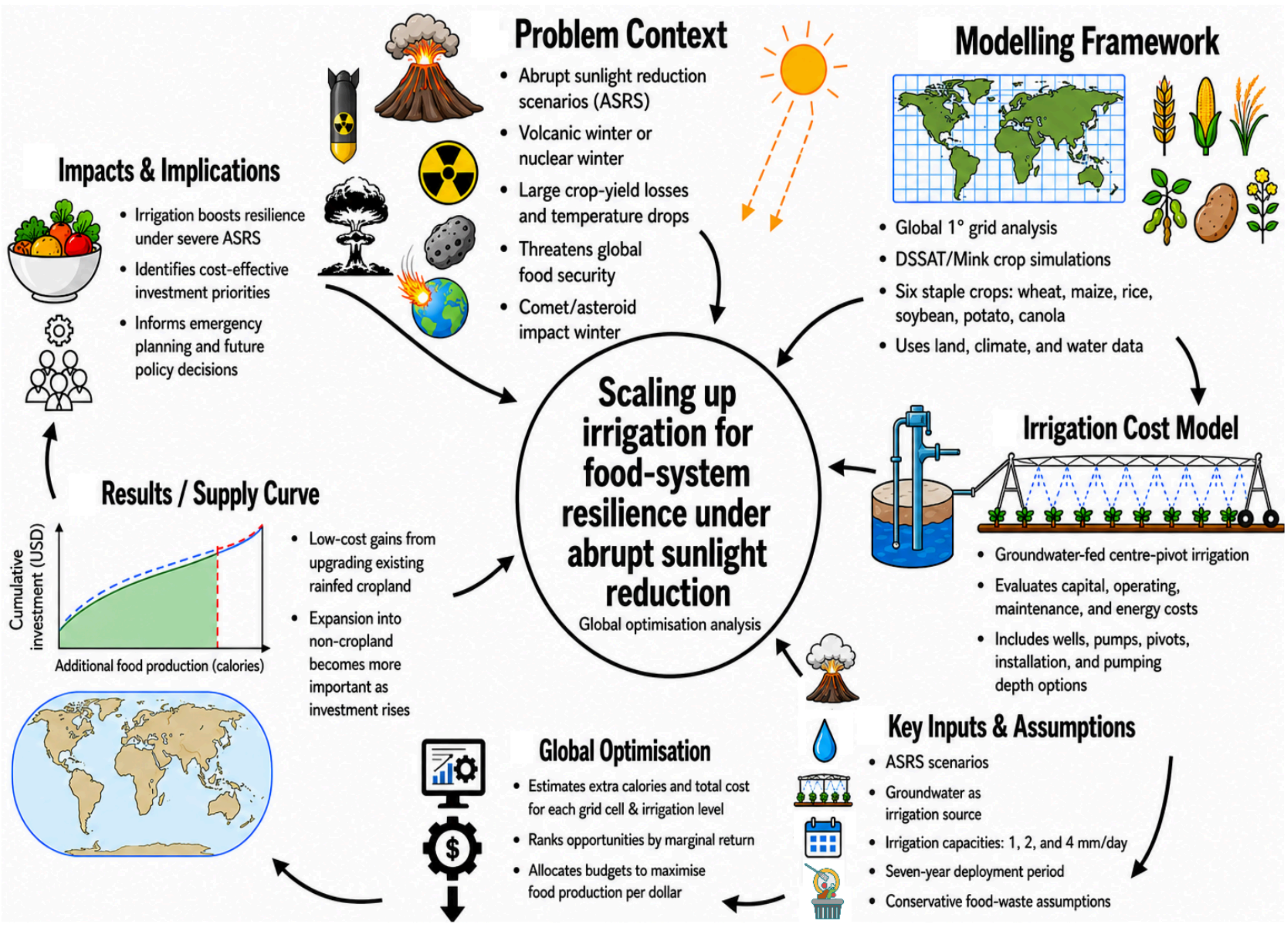

Symbol	Value	Definition	Units	Symbol	Value	Definition	Units
Y_T		Total caloric yield over the analysis window	kcal ha^{-1}	N	7	Number of analysis years (y2–y8)	years
k	3.4×10^6	Grain-equivalent caloric density	kcal t^{-1}	y		Annual yield per hectare (Eq. 1)	t ha^{-1} yr^{-1}
C_f		Annual cultivation cost per hectare (Eq. 2)	USD ha^{-1} yr^{-1}	C_F		Total cultivation cost over N years (Eq. 3)	USD ha^{-1}
C_p		One-time land preparation cost by land-cover type	USD ha^{-1}	I		Irrigation capacity; $I \in \{1, 2, 4\}$	mm day^{-1}
Q_w		Well capacity	m^3 day^{-1} per well	m	10	mm-to-m^3 per ha conversion factor	m^3 ha^{-1} mm^{-1}
W_h		Wells per hectare (Eq. 4)	wells ha^{-1}	d		Water-table depth (absolute value)	m
r	0.10	Cost-of-capital (interest) rate	—	$C_{capex/ha}$		Irrigation CAPEX per hectare (Eq. 5)	USD ha^{-1}
W_T		Total irrigation water over the time horizon	mm	C_{ca}		Annualised CAPEX per ha per year (Eq. 6)	USD ha^{-1} yr^{-1}
$C_{op,yr}$		Annual operating cost per hectare (Eq. 8)	USD ha^{-1} yr^{-1}	Q		Annual water applied per hectare (Eq. 7)	m^3 ha^{-1} yr^{-1}
C_I		Total irrigation cost over the horizon (Eq. 10)	USD ha^{-1}	C_m		Annual maintenance cost per hectare (Eq. 9)	USD ha^{-1} yr^{-1}
Greek symbols							
η	0.70	Pump efficiency	—	ΔC_i		Incremental cost of segment i	USD
ΔP_i		Incremental production of segment i	kcal				
Abbreviations							
ASRS		Abrupt sunlight-reduction scenario	—	DSSAT		Decision Support System for Agrotechnology Transfer	—

CAPEX	Capital expenditure	USD	FAO	Food and Agriculture Organisation of the United Nations	—
ECe	Electrical conductivity of the saturation extract	dS m^{-1}	Mha	Million hectares	10^6 ha
Gt	Gigatonne	10^9 t	Tg	Teragram (soot mass unit)	10^{12} g
SPAM	Spatial Production Allocation Model	—	USD	United States dollar	
TDS	Total dissolved solids	g L^{-1}	y2–y8	Analysis years 2–8 of the ASRS scenario	—
WTD	Water-table depth	m	SDG	Sustainable Development Goal	

1 Introduction

ASRSs, such as volcanic winter, impact winter, or nuclear winter resulting from nuclear war and the burning of cities, represent particularly alarming threats to global food security. Stratospheric aerosols can remain aloft for several years, blocking incoming sunlight, cooling the Earth's surface, and shortening growing seasons worldwide (Coupe et al., 2019; Robock, 2010). Crop yields would be severely affected, particularly in mid- to high-latitude regions of the Northern Hemisphere, with the potential to trigger widespread famine on a global scale (Jägermeyr et al., 2020; Xia et al., 2022).

A range of food solutions have been proposed to address the impacts of such scenarios, including seaweed cultivation (Jehn et al., 2024), greenhouses (Alvarado et al., 2020), lignocellulosic sugar production (Throup et al., 2022), methane single-cell protein (García Martínez et al., 2022), leaf protein concentrate (Fist et al., 2021), frost-tolerant outdoor crops (Wilson et al., 2023), and fat synthesis (García Martínez et al., 2025). Rivers et al. (2024) demonstrate that through the combined adoption of such adaptive strategies, alongside food waste reduction and redirecting animal feed to human consumption, the risk of mass starvation during a worst-case ASRS scenario involving 150 Tg of soot can be substantially reduced.

Outdoor cultivation remains feasible in certain regions even under severe ASRS conditions, particularly in tropical and southern temperate latitudes where reductions in temperature and growing season length are less pronounced (Xia et al., 2022). The conversion of non-agricultural lands, including herbaceous, shrub, barren, and young secondary forest areas, into winter wheat farmland, referred to hereafter as cropland expansion, was examined by Monteiro et al. (2024). The authors applied a process-based crop growth model to identify productive lands with mean productivity exceeding 1 t/ha/year during the ASRS, and estimated the physical feasibility of clearing and cultivating up to approximately 1.45 billion hectares using global construction and forestry machinery fleets under various equipment deployment scenarios. They found that cropland expansion could contribute substantially to caloric production following an ASRS, though it remains constrained by equipment availability and coordination challenges, and carries significant ecological consequences.

However, that assessment considered land clearing without accounting for irrigation infrastructure. Under ASRS conditions, water stress remains a significant determinant of yields, and irrigation can become economically worthwhile even in areas where it would not be viable under baseline climate conditions, owing to the increased marginal value of calories. Irrigation systems rely on wells, pumps, and water conveyance technologies, and their deployment is governed by capital availability, well-drilling capacity, and water availability and quality (Food and Agriculture Organization of the United Nations [FAO], 2011; Frenken, 2012; Hassani et al., 2020; UNESCO International Hydrological Program [UNESCO-IHP], 2013). Irrigation could prove especially beneficial when combined with crop shifting and cropland expansion, yet no globally integrated optimisation model for this combination currently exists.

Unlike the sudden decline in solar irradiance characteristic of ASRSs, anthropogenic climate change is gradually altering temperatures and the hydroclimate regime, increasing evapotranspiration stress and shifting drought and heat risk patterns in ways that are progressively exposing rainfed agricultural systems and tightening regional water balances (Intergovernmental Panel on Climate Change [IPCC], 2022). In this context, irrigation is widely regarded as an essential adaptation strategy, provided that freshwater can be mobilised without compromising ecosystem integrity, downstream communities, or the needs of future generations. However, irrigation development faces several binding constraints, including capital availability, energy requirements for water lifting, drilling capacity, groundwater reserves, and water quality concerns such as salinity and the risk of soil salinisation (FAO, 2011; Hassani et al., 2020). The appropriate tools for assessing long-run climate risk in this domain are spatially explicit models that estimate irrigation expansion potential, associated water requirements, and supply shortfalls (e.g., Elliott et al., 2014; Jägermeyr et al., 2016; Rosa et al., 2020; Rosa, 2022). Here, we address an analogous problem in a fundamentally different context.

We develop a global, spatial framework to prioritise groundwater-based irrigation investment across existing cropland and candidate expansion land under baseline and 150-Tg soot ASRS climates, using gridded crop simulations to translate alternative irrigation choices into calories, costs, and deployment-relevant constraints (salinity, land cover, clearing and drilling assumptions). We apply it to identify where limited budgets buy the most food and to quantify global supply curves and deployment trajectories for emergency planning. In doing so, we extend the evidence base for Sustainable Development Goal (SDG) 2 (Zero Hunger) into the tail of the risk distribution for food system disruptions.

2 Methods

2.1 Data

2.1.1 Climate Scenario

In the present study, we examine an extreme ASRS generated by the injection of 150 Tg of soot into the stratosphere, based on climate model simulations conducted by Coupe et al. (2019). The soot injection produces multi-year reductions in incoming solar radiation and surface temperature, with conditions recovering over approximately ten years. The ASRS onset in the simulations occurs in May of year one, and years two through eight (y2–y8) constitute our primary period of analysis.

2.1.2 Mink Crop Model and Yield Data

The Mink global gridded crop framework (Robertson, 2017) integrates the DSSAT crop physiology model with global gridded soil and climate data, incorporating spatially explicit fields of climate variables, including temperature, precipitation, solar radiation, and soil characteristics, specified at each grid cell on each time step. While Monteiro et al. (2024) employ a single cold-tolerant winter wheat cultivar, our analysis using Mink is multicrop; six staple crops are examined, namely wheat, maize, rice, potato, soybean, and canola (rapeseed), with the most productive staple selected for each grid cell after accounting for crop switching costs (Blouin et al., 2025). DSSAT, operating within the Mink framework, uses daily weather sequences and a crop physiology model that includes vernalisation for appropriate crops, with scenarios configured following Blouin et al. (2025). Nitrogen application rates are held constant throughout. The native resolution of Mink is 1.875° × 1.25°; interpolation to 1° × 1° grid cells is applied only for the irrigation optimisation component of the analysis.

For each grid cell and each year, Mink provides the yield without irrigation, the yield increment attributable to irrigation, and total irrigation water consumption at application capacities of 1, 2, and 4 mm day^{-1}. Irrigation is triggered whenever available soil water falls below 70% of field capacity (i.e., before water stress starts) and ceases once available water exceeds that threshold again or the daily maximum application rate is reached. In the optimisation framework, all relevant quantities are summed over years two through eight.

2.1.3 Land Cover, Slope, and Expansion Types

Land cover data for non-agricultural expansion are drawn from the EarthEnv Global 1 km Consensus Land Cover map (Tuanmu & Jetz, 2014), aggregated to 1° resolution, where each grid cell is assigned the proportional coverage of herbaceous vegetation, shrubland, and bare soil. Forest age is obtained from the Global Forest Age dataset (version 1.1) (Poulter et al., 2019), which provides the fraction of young forest in each grid cell, retained here as the available proportion for expansion purposes. Following Monteiro et al. (2024), expansion is permitted across four land cover classes, namely herbaceous vegetation, shrubland, bare soil, and young forest, while expansion is excluded from existing cropland, open water, ice, built-up land, flooded vegetation, older forests, and steeper land.

2.1.4 Soil Salinity and Saline Groundwater

Soil salinity data are derived from the predicted global surface electrical conductivity of the saturation extract (ECe) provided by Hassani et al. (2020). The mean annual ECe surface is used here, with soils classified as problematic where values exceed 7.8 dS/m, a threshold associated with approximately 5 g/L of total dissolved solids and a wheat yield reduction of around 13%, in accordance with Food and Agriculture Organisation guidelines (FAO, 1985).

ECe values for each underlying pixel are aggregated to 1° grid cells, and the proportion of pixels exceeding the salinity threshold is defined as the saline soil fraction, which reduces the usable land area available for expansion. Existing cropland is retained at its full land area, as current management practices are assumed capable of addressing any associated salinity issues. Saline groundwater is modelled separately by constructing polygons derived from the global groundwater quality database of the IHP Water Information Network System (IHP-WINS) Areas of Saline Groundwater (UNESCO Intergovernmental Hydrological Programme, 2024). New groundwater-based irrigation investment is prohibited within areas delineated by these polygons, while existing irrigated cropland within the same areas is permitted to continue operating.

2.1.5 Staple Scaling

Although six staple crop types are included in the optimisation, actual agricultural land use and food consumption depend on a broader range of crops beyond these staples. Treating 100% of all agricultural and expansion land as candidates for staple irrigation would substantially overestimate the available area, given that the proportion of agricultural land dedicated to non-staple crops considerably exceeds that accounted for in the present analysis. Accordingly, land area scaling is applied using the SPAM 2020 Physical Crop Areas dataset (Yu et al., 2020) to ensure a more realistic representation of staple crop land allocation.

Current agricultural areas: For each grid cell, the proportion of total rainfed and irrigated land dedicated to each staple crop relative to all crops classified in SPAM is calculated, and these proportions are subsequently multiplied by the total hectares per cell to derive staple-specific land areas.

Expansion areas (all non-cropland categories): Since SPAM cannot provide crop mixture data for non-cropland areas, it is not possible to derive staple-specific fractions at the cell level for expansion lands. Instead, a single universal scaling constant is applied to all expansion areas, defined as the ratio of total staple crop area to total crop area in SPAM, ensuring that expansion estimates remain conservative across all locations. This approach is necessary to prevent overestimation of staple area in cells that also contain non-staple crops. Figure 1 illustrates the distinction between the cell-based cropping fraction used for existing agricultural land and the global expansion weighting of approximately 51% applied to non-cropland areas.

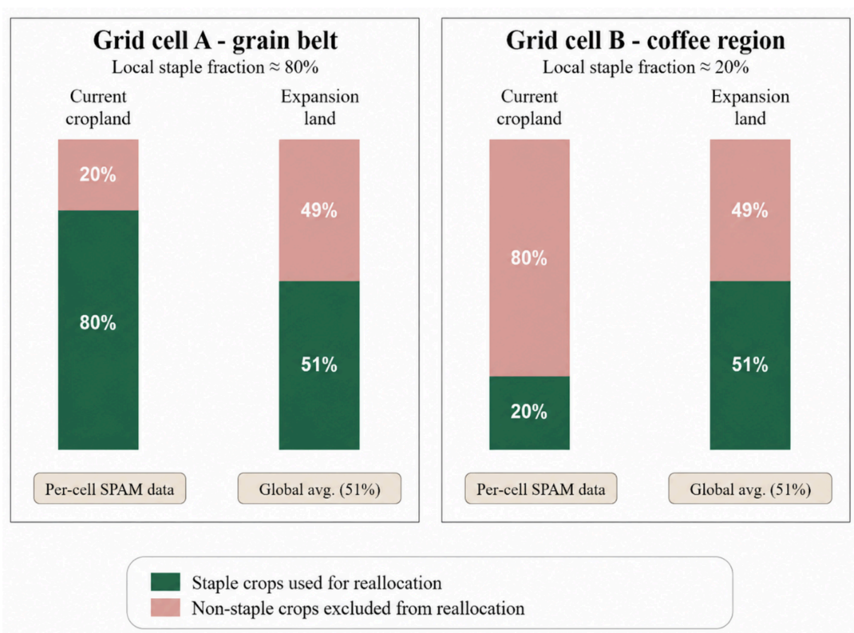

Figure 1. Staple versus non-staple allocation for cropland and expansion in two example cells. Schematic of staple fractions for current cropland (per-cell SPAM) versus expansion land (global average: 51%). Teal, staple crops (calculated); pink, non-staple crops (not calculated).

2.1.6 Cost Parameters

Table 1: Key parameters and constants used in the model, with sources justified in the appendix unless otherwise noted.

Parameter	Symbol	Value	Unit	Source
Well cost per metre drilled (drilling and casing cost)	C_{wm}	355	USD m^{-1}	
Centre-pivot and installation cost	C_{total}	1,776	USD ha^{-1}	
Fixed conveyance cost	C_{fx}	0.0098	USD m^{-3}	
Maintenance per well per metre	C_{md}	21.6	USD well^{-1} m^{-1} yr^{-1}	
Per-hectare irrigation maintenance	C_{mi}	53	USD ha^{-1} yr^{-1}	
Pump-depth offset	d_0	20	m	
Variable yield-proportional cost	C_v	171	USD t^{-1} yr^{-1}	Estimated from USDA Commodity Costs and Returns Data, wheat country average for 2025 (USDA ERS, 2026).
Depth-dependent pumping cost	C_d	0.0015	USD m^{-3} m^{-1}	
Variable pump-to-pivot water-moving cost	C_{mv}	0.0187	USD m^{-3}	
Maintenance per pump	C_{mp}	2,488	USD well^{-1} yr^{-1}	
Centre-pivot coverage factor	f_{pv}	0.785	—	Geometric fraction of a square field irrigated by an inscribed centre-pivot circle
Fixed annual cultivation cost	C_b	400	USD ha^{-1} yr^{-1}	Estimated from USDA Commodity Costs and Returns Data, wheat country average for 2025 (USDA ERS, 2026).

All new irrigation is assumed to be ground-fed with centre-pivot distribution systems. Drip irrigation, furrow or flood irrigation, travelling gun systems, and aerial irrigation are not represented. Centre-pivot systems were selected for future irrigation expansion because they apply water efficiently and effectively. Centre-pivot /sprinkler systems also tend to use water more efficiently than surface methods. Under reasonable management, reported application efficiencies are about 85% for sprinkler systems versus about 65% for furrow irrigation (Lamm & Trooien, 2003). Field tests under a range of climatic conditions show that a standard centre-pivot system typically achieves a coefficient of uniformity of 74–90% (average approximately 86%) (Al-Ghobari & Dewidar, 2021). Drip and micro-irrigation systems can reach higher efficiencies but carry considerably higher installation and maintenance costs per hectare.

Allocation of new irrigation systems in our model is constrained to groundwater-irrigated centre-pivots for simplicity of implementation. It is not possible to estimate how much surface water would be available under an ASRS scenario, because precipitation, runoff, snowmelt timing and lake water levels would all change, and we do not currently have estimates of post-disaster river flow rates. Moreover, even assuming that future surface water availability could be predicted, there would still be the problem of estimating the effect of large-scale withdrawals from rivers and lakes. In contrast to surface water, the amount of groundwater available for irrigation is better known and is not strongly affected by short-term climate perturbations, so the allocation is made for groundwater only. This approach is conservative with respect to future scale-up of irrigated areas compared to what could be achieved if other irrigation techniques were expanded alongside groundwater.

Capital costs include installed well costs and installed centre-pivot equipment, financed at an annual interest rate of 10%, consistent with discount rates applied by the World Bank and Asian Development Bank for comparable projects (Zhuang et al., 2007; Castillo & Zhangallimbay, 2022). Operating costs are calculated as a function of water volume and lifting depth, while maintenance costs incorporate depth-related well components and a per-hectare irrigation maintenance charge. In addition to irrigation infrastructure costs, crop operating costs are included for each management level, comprising a fixed farming cost per hectare and an additional component proportional to yield.

Cultivation costs

We represent cultivation costs per hectare as the sum of a fixed annual component and a yield-proportional annual component. Let Y_T be the total caloric yield over the analysis window (kcal ha^{-1}), N the number of years, and $k = 3.4\times10^6$ kcal t^{-1} (grain-equivalent). The annual yield in tonnes per hectare is

$$y = \frac{Y_T/N}{k}. \quad (1)$$

Let C_b be the fixed annual cultivation cost and C_v the variable yield-proportional cost. We model the annual cultivation cost as follows:

$$C_f = C_b + C_v y, \quad (2)$$

and the total cultivation cost is

$$C_F = N\, C_f. \quad (3)$$

For expansion of cropland, a one-time land preparation cost C_p (USD ha^{-1}) is applied by land-cover type (C_p = 0 for existing cropland; \$2,450 ha^{-1} for herbaceous vegetation, shrubs, and barren; \$7,350 ha^{-1} for young forest). We anchor land conversion costs on BrasilAgro, a company whose business is acquiring and developing agricultural land in Brazil, which reports investing R\$115.7 million to bring 51,662 hectares into grain production through June 2014, together with R\$26.8 million in associated buildings, or approximately \$1,000/ha in current terms (BrasilAgro, 2014). We take this as the minimum for non-forested land (BrasilAgro's holdings are concentrated in the Brazilian Cerrado). Because Brazilian costs are low, we obtain a high-income upper bound by scaling with the ratio of construction price level indices reported by the World Bank's International Comparison Program (2021) for the US and Brazil, which provides a factor of six. For forested land we apply a further factor of three, the approximate ratio of heavily to lightly forested clearing costs in United States commercial land clearing. This yields \$1,000–\$6,000/ha for herbaceous, shrub, and barren cover and \$3,000–\$18,000/ha for young forest, with central estimates of \$2,450/ha and \$7,350/ha respectively, taken as geometric means.

Irrigation costs (wells, pumps, and centre pivots)

For an irrigation capacity $I \in \{1, 2, 4\}$ mm day^{-1}, let η be pump efficiency, Q_w well capacity (m^3 day^{-1} per well), D being diameter of well, v being entrance velocity to the casing, l and m = 10 the conversion from mm to m^3 ha^{-1} (1 mm over 1 ha = 10 m^3). Wells per hectare are

$$w_h = \frac{I\, m}{\eta\, Q_w}. \quad (4)$$

Where, Q_w is calculated using a well diameter D of 8 in. (Western Drilling, 2024) and entrance velocity to the casing is 0.46 m/s (Ballard, 2017; Turnbull, 2026).

Let the C_{total} centre-pivot and installation cost, w_h wells per hectare, d water-table depth, d_0 pump-depth offset, C_{wm} well cost per metre drilled, C_{wb} well base cost. We model irrigation capital expenditure per hectare as

$$C_c/\mathrm{ha} = \mathrm{C_{wm}}\,(d + d_0)\cdot w_h + C_{\mathrm{total}}. \quad (5)$$

Let r cost-of-capital (interest) rate, capital expenditure is annualized over the horizon with a cost-of-capital term:

$$C_{ca} = \frac{C_c/ha}{N} + r\,\frac{C_c}{ha}, r = 0.10 \quad (6)$$

Let W_T total irrigation water over the time horizon, annual water applied (m^3 ha^{-1} yr^{-1}) is

$$Q = \frac{W_T m}{N\eta}. \quad (7)$$

Let C_d depth-dependent pumping cost, C_{fx} fixed conveyance cost, C_{mv} variable pump-to-pivot water-moving cost, Q annual water applied per hectare, operating (pumping and conveyance) cost per hectare per year is

$$C_{op,yr} = \left(C_d\left(d + d_0\right) + C_{fx} + C_{mv}\right)Q, \quad (8)$$

Let C_{md} maintenance per well per metre, C_{mp} maintenance per pump, C_{mi} per-hectare irrigation maintenance, maintenance per hectare per year is (see Appendix A for a derivation)

$$C_{\mathrm{m}} = (C_{\mathrm{md}}\, d + C_{\mathrm{mp}}) \cdot (24Q)/(8000\cdot Q_{\mathrm{w}}) + C_{\mathrm{mi}}. \quad (9)$$

Let C_{ca} annualised CAPEX per ha per year, $C_{op,yr}$ annual operating cost per hectare, C_m annual maintenance cost per hectare, total irrigation cost over the horizon is

$$C_I = N\left(C_{ca} + C_{op,yr} + C_m\right). \quad (10)$$

The numerical values of all cost parameters, together with the equations used to derive them from primary sources, are presented in Appendix A. The sensitivity of the results to individual cost parameters is reported in Section 3.4.

2.1.7 Energy requirements for groundwater lifting

We also report an order-of-magnitude estimate of the energy required to lift the irrigation water implied by the model, using the same per-cell annual applied water, irrigated hectarage (centre-pivot coverage for new irrigation; full area for existing irrigated cropland), and static lift head $H_{static} = |WTD| + 20$ m (WTD = water table depth) as in the pumping-cost parameterisation. For an illustrative high-ambition allocation scenario, the implied annual volume of groundwater lifted would be approximately 690 km^3/yr, with a volume-weighted mean lift of roughly 43 m, corresponding to an implied theoretical minimum hydraulic work cost of approximately 80 TWh/yr of static hydraulic work. To produce a more realistic estimate of fuel consumption for pumping, a friction loss term equal to approximately 25% of the static head is incorporated, giving an effective fluid head of roughly 1.25 times the static head, accounting for losses from pipes, screens, fittings, and related components. A centrifugal pump efficiency of 70% is assumed for converting hydraulic head to shaft work. For the engine itself, a conservatively low chemical-to-shaft work efficiency of approximately 30% is adopted to reflect seasonal average and off-peak operating conditions, rather than the maximum brake thermal efficiency of around 40% achievable under optimal conditions. At a lower heating value for diesel fuel of approximately 9.9 kWh/L (IPCC, 2019), this yields a fuel requirement of roughly 48 billion litres per year, equivalent to approximately 3.0% of global gasoline and diesel demand, estimated by the International Energy Agency at approximately 27–28 million barrels per day, or around 1.6×10^{12} litres per year, during the 2020s (IEA, 2024). In reality, demand would likely be lower as some systems would use electricity for pumping.

2.2 Optimisation Model

2.2.1 Farming and Irrigation Levels

For each combination of spatial entries, defined by grid cell and land cover type, the model includes a finite set of management options. Management level 0 represents a non-intervention option in which land is left idle. Management level R refers to rainfed farming of the entire area at baseline yields. Levels I1, I2, and I4 correspond to centre-pivot irrigation of 78.5% of the entry area at maximum application rates of 1, 2, and 4 mm per day respectively, with the four corner sections excluded from irrigation. Levels RI1, RI2, and RI4 farm the full parcel: centre-pivot irrigation of the pivot coverage area at 1, 2, or 4 mm d^{-1}, with the remaining corner area rainfed. Level C applies to already irrigated cropland and involves farming of the entire area at yields corresponding to the maximum irrigation intensity of 4 mm per day. For each management level, crop-model yield and irrigation water demand are combined with cost assumptions to estimate food-energy production and the associated land-preparation, farming, and irrigation-well installation, operation, and maintenance costs.

2.2.2 Convex-Hull Preprocessing and Segment Construction

Each feasible combination of farm and irrigation system management is assigned costs and total food production per scenario period within each grid cell and land cover type, with irrigation costs that increase with groundwater depth, exclusion of cells lacking water-table data, exclusion of additional irrigation in saline groundwater grid cells while permitting rainfed farming, a reduction in expansion hectares for saline soils, and a fixed set of pivot and irrigation intensity levels. All feasible management combinations for each cell–land-cover entry (none, rainfed only, irrigation-pivot intensities, and rainfed plus irrigation) are evaluated as cost–production pairs over the analysis window. Dominated alternatives, those that yield less food at equal or higher cost than another option, are discarded, and an upper convex hull is constructed from the remaining non-dominated points so that only options along the frontier of increasing cost and increasing production are retained. Adjacent hull points define upgrade segments, each characterised by a starting level, an endpoint, incremental cost (USD), incremental production (kcal), and a return on investment (ROI) = Δproduction/Δcost. Figure 2 illustrates this screening for one example rainfed-cropland cell, using absolute costs and staple kilocalories from the crop and infrastructure parameterisation; the same procedure is applied to every grid cell and land-cover type before global budget allocation.

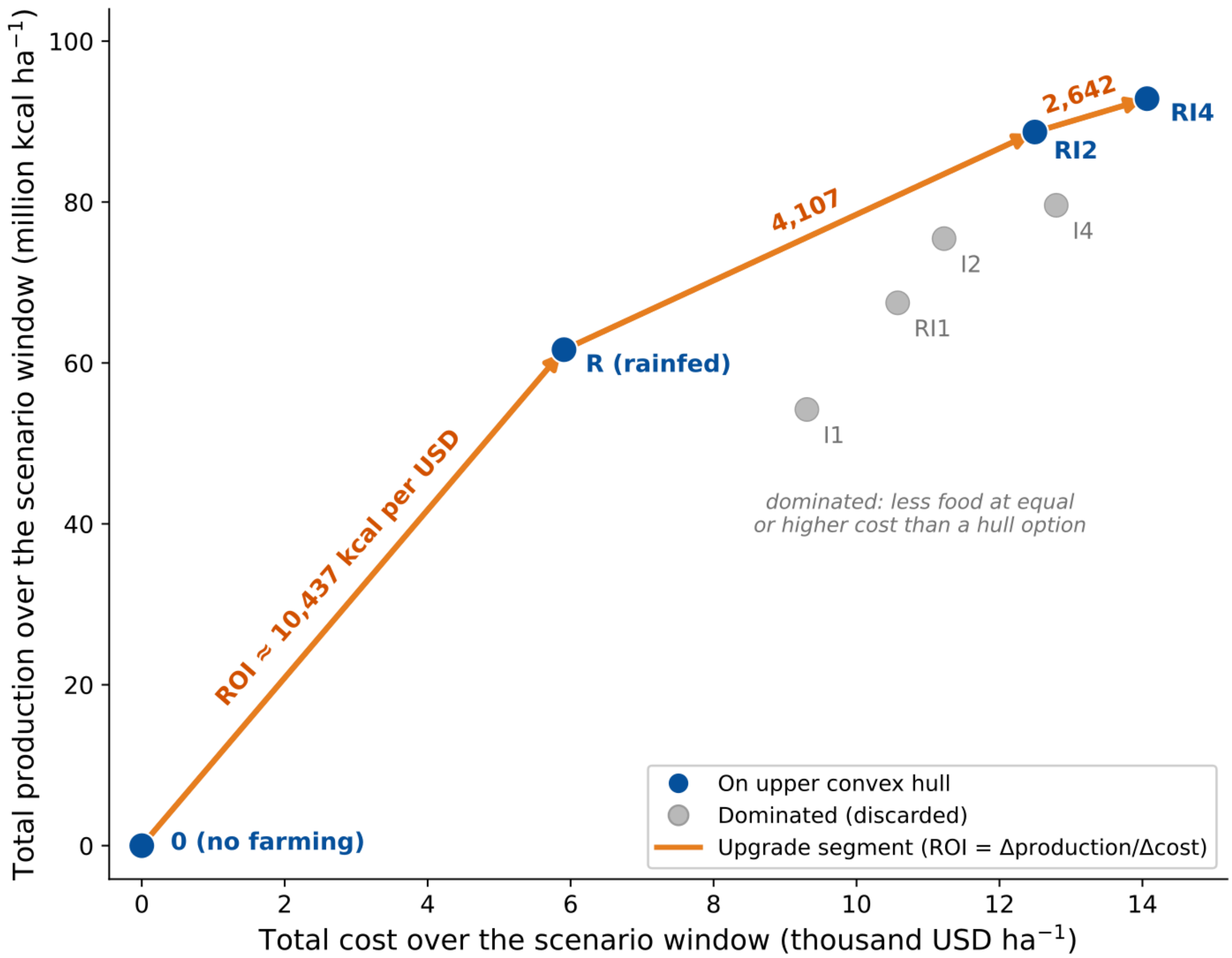

Figure 2. Convex-hull preprocessing for a rainfed-cropland entry (grid cell at 22°N, 104°W, Mexico). Each point is one management level. Gray points indicate dominated options (less food at equal or higher cost than an option on the hull), blue points form the upper convex hull, and orange arrows indicate the marginal upgrade segments retained by the optimiser.

2.2.3 Global Budget Allocation and optimisation Flow

Figure 3 shows how the optimisation process was carried out. We retain the points on the upper convex envelope, then define segments between adjacent retained vertices with ΔC, ΔP, and $ROI = \Delta P/\Delta C$. All segments are pooled globally and sorted by ascending marginal cost per unit of production.

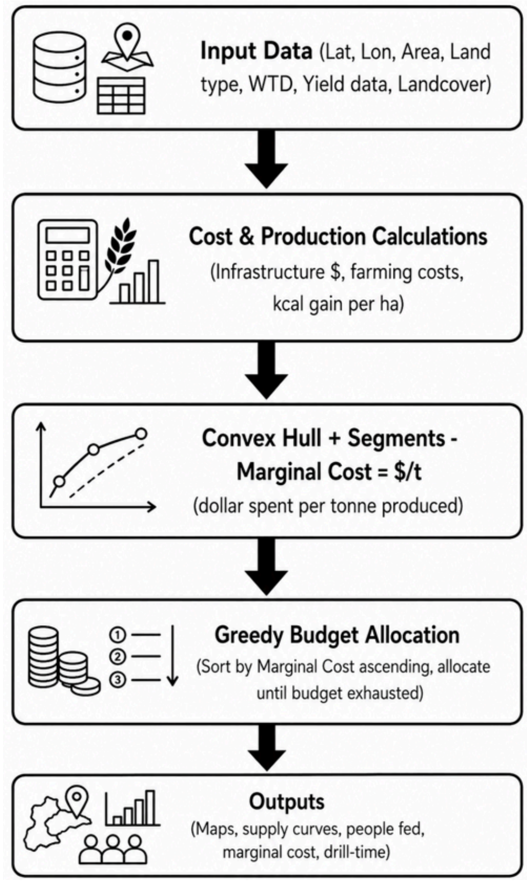

Figure 3: Optimisation algorithm

All entries start at level 0. The allocator walks through cost-per-tonne-ranked segments and accepts one only if its cost fits the remaining budget; accepted segments update state, cost, production, summary totals, and allocation order.

2.2.4 Drilling Units and Irrigated-Area Progress Curves

The analysis also accounts for drilling capacity across three parallel rig categories, namely agricultural, oil and gas, and residential or lighter equipment, each assigned a constant penetration rate in metres per day (275 ft/day for AG and RES, and 1000 ft/day for oil and gas wells) (Tidal Petroleum, 2026; Cascade Environmental, 2020). Prior to budget allocation, the number of rigs of each type is specified, denoted as AG for agricultural wells, OG for oil and gas wells, and RES for residential wells, and this determines the rate of drilling per unit of well footage allocated. Global estimates of available drilling rigs were derived by dividing annual market revenue by the average unit cost and multiplying by an average equipment lifespan of 15 years, yielding approximately 10,493 agricultural well-drilling rigs, 1,479 oil and gas rigs, and 42,419 residential well-drilling rigs (see Appendix B).

Let A denote the land-cover entry area (ha), f_{pivot} the fraction of that entry under the centre pivot ($f_{pivot} = \pi/4$), and

$$A_{irr} = f_{pivot} A \quad (11)$$

the pivot-irrigated area (ha) for a new irrigation upgrade. Let $I \in \{1, 2, 4\}\ mm\ day^{-1}$ be the irrigation capacity, η the fraction of pumped water assumed to reach the soil, Q_{well} the maximum well discharge ($m^3\ day^{-1}$ per well), and m the conversion from applied depth to volume per hectare ($m^3\ ha^{-1}\ mm^{-1}$). Wells per hectare are

$$w_h = \frac{Im}{\eta Q_{well}}\ .\ (12)$$

and the implied well count on the irrigated footprint is

$$N_{wells} = w_h A_{irr}\ .\ \ (13)$$

Let $d = |WTD|$ be the absolute water-table depth (m), d_0 a fixed pump-depth offset (m), and

$$D = max(d + d_0, \varepsilon) \quad (14)$$

the representative drilled depth per well (m), with a small numerical lower bound $\varepsilon > 0$.

For rig classes $i \in \{AG, OG, RES\}$, let v_i be the constant penetration rate ($m\ day^{-1}$) and N_i the number of parallel rigs (units) of that class. If that class alone completed all wells, the calendar time would be

$$T_i = \frac{D}{v_i} \frac{N_{wells}}{N_i}\ .\quad (15)$$

With all three classes working in parallel on the same cell scope, we use the harmonic-style composition of independent completion rates $1/T_i$:

$$T_{cell} = \frac{1}{\sum_{i:T_i>0} \frac{1}{T_i}}\ .\quad (16)$$

2.3 Assumptions and Calibration

In the following, we state and justify several key assumptions and calibrations.

2.3.1 Production Targets and Marginal Costs

Food-system studies such as Hinge et al. (2026) show that, after multi-year crop shocks, cereal prices can rise by an order of magnitude or more. In this paper, we estimate the cost of production, not the equilibrium price. The purpose is to show how large groundwater centre-pivot irrigation should be, and roughly how costly, if used as one resilience option alongside relocating crops on existing cropland and expanding planted area without irrigation. Since the cost is calculated as an average over 7 years, and production is lower in the first few years, the equilibrium prices will be considerably higher in the first years than the 7-year average cost. Compared with economy-wide food-system targets that include non-staple crops and other resilient foods, the irrigation supply curve here is narrower in scope: it covers only six staple crops and groundwater centre-pivot expansion and continued use. Therefore, at any given marginal cost, the dry carbohydrate quantity on this curve is smaller than would be expected from those broader food-system goals.

We therefore use staple-oriented (wheat, maize, rice, soybean, potatoes, and canola modelled, but other grains are included in staples) benchmarks (e.g. ~2.8 Gt yr^{-1} dry carbohydrate) as the comparison point on the curve, while treating Hinge et al. (2026) as economic context for order-of-magnitude marginal prices under shock. The value of 2.8 Gt/yr dry carbohydrate, estimated from the FAOSTAT value of just over 3.1 billion tonnes of cereals produced in 2023 (the latest year with full coverage) converted at the reported caloric content of each cereal product listed within FAOSTAT (approximately 3,500 kcal/kg) (FAO, 2026).

Under a 150-Tg ASRS, pasture and forage availability for livestock could experience near-total failure, with losses estimated at approximately 85% in such extreme scenarios (Xia et al., 2022). Additional grazing land would also be displaced by cropland expansion. Increased use of crop residues could partially offset grass losses, though only to a limited degree. Reductions in food waste, biofuel production, and feed consumed by non-ruminants are also anticipated (Rivers et al., 2024). Nevertheless, a severe loss of livestock feed derived from human-inedible sources would likely result in some diversion of human-edible food to ruminant feeding.

2.3.2 Food Waste and People-Fed Calculation

The number of people fed is derived by converting annual food-energy production from the model into a population equivalent, using a standard daily energy intake of 2,100 kilocalories per person per day, and then reducing it by an estimated loss-and-waste factor applied between the farm gate and the consumer. A loss-and-waste factor of 0.29 is used, consistent with global estimates that account for both pre-market food losses and post-market consumer waste (Gustavsson et al., 2011; FAO, 2019; United Nations

Environment Programme [UNEP], 2021). We do not assume that the loss-and-waste factor would decline sharply under an abrupt sunlight reduction scenario, since in the absence of extreme food shortages driven by irrigation expansion, additional cropland, and other adaptive measures, food prices would likely not escalate to levels at which waste reduction becomes as substantial as considered in previous work.

3 Results

Because the results depend on the chosen budgets and configurations, we outline the main output types and how they should be interpreted.

3.1 Feasibility of drilling the new wells in time

Before discussing our findings on land and economics, one question must be answered first: whether the new wells assumed in the large-scale expansion scenario could be drilled within a timeframe that would contribute to disaster avoidance. Figure C1 in Appendix C is therefore a test of drilling capacity rather than a complete project schedule.

Figure C1 shows cumulative newly irrigated area (ha) versus cumulative well-drilling time (days), with projects ordered by the optimiser (highest incremental food per dollar first). Each step adds the pivot-irrigated area associated with new wells; time is estimated from well depth (|WTD| + 20 m), the number of wells required for the chosen intensity (1/2/4 mm d^{-1}), and assumed parallel drilling capacity (agricultural, oil and gas, and residential fleets at fixed metres-per-day rates). Current cropland is drilled before expansion. The x-axis counts continuous productive drilling only, excluding mobilisation, transport between sites, and weather downtime. The base rates assume 56 hours of operation per week (see Appendix B5); in the event of catastrophe, this could be increased significantly (for example, using lighting to operate for around 80% of the week would allow roughly 134 hours per week). This could leave additional time for delays beyond drilling itself. Access roads and other developments are already included in the land preparation cost and are not expected to govern the schedule of the clearing phase. The fleet sizes are likewise conservative relative to the additional drilling units that could be produced in the event of catastrophe.

3.2 Global Irrigation Allocation

Figure 4 isolates optimisation outcomes for existing rainfed cropland only. Most cells remain in the rainfed-only category (light blue), while a smaller subset is upgraded to new irrigation at 1, 2, or 4 mm d^{-1}(yellow, orange, and purple), indicating where irrigation yields sufficient marginal return under the budget constraint. Upgrades cluster in regions where expected yield gains are high relative to costs (including local yield response and groundwater depth), whereas most cells remain not upgraded because their marginal benefit is lower than competing opportunities in the global allocation. The legend reports the number of hectares assigned to each class and also marks regions with saline groundwater where irrigation is excluded and cropland remains rainfed only (gray shading).

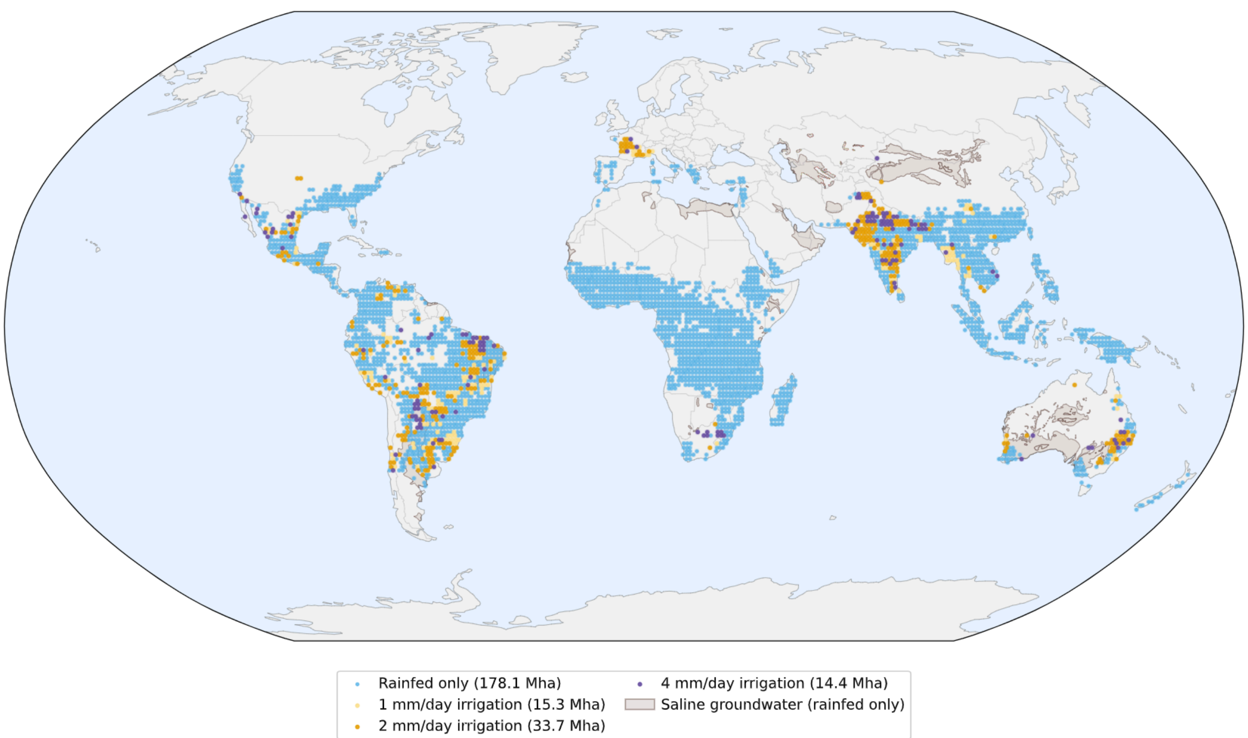

Figure 4. Current rainfed cropland decisions under the 150-Tg ASRS case (analysis years 2–8) with total investment budget of $8.935 trillion.

Figure 5 shows where the optimal allocation expands onto non-cropland and how intensively that land is managed. Most selected expansion is rainfed only (~200 Mha), concentrated in the Amazon basin, Central Africa, and parts of Southeast Asia and northern Australia. Irrigated expansion is smaller but still substantial: about 17 Mha at 1 mm d^{-1}, 89 Mha at 2 mm d^{-1}, and 103 Mha at 4 mm d^{-1}, with clearer clusters in parts of Brazil, Australia, and South Asia. Saline-groundwater zones (shaded) remain rainfed-only, and at the $8.935 trillion allocation, about 39 Mha is cultivated in saline-groundwater zones (26 Mha rainfed expansion); areas with predominantly saline soils are marked separately.

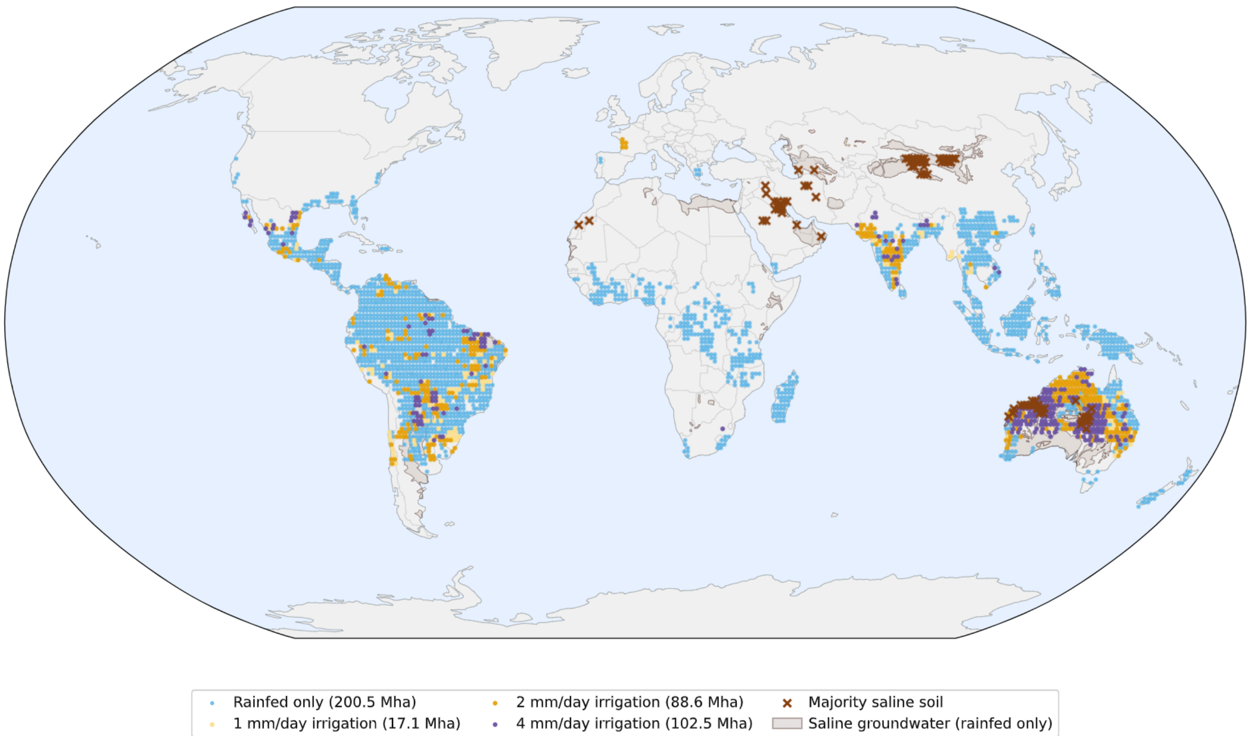

Figure 5. Expansion-land decisions under the 150-Tg ASRS case (analysis years 2–8), with a total investment budget of $8.935 trillion.

Figure C2 (Appendix C) shows optimisation outcomes for already-irrigated cropland cells. Fifty-eight percent of existing irrigated staple cropland area is retained (blue), indicating that most of the existing irrigation infrastructure remains economically valuable under ASRS conditions (except at higher latitudes, where the climate impact is most severe) and is retained rather than abandoned. Because these areas do not require new irrigation installation, they provide relatively low-cost maintained production compared with developing new infrastructure elsewhere.

Figure C3 (Appendix C) summarises where the optimal allocation converts non-cropland to rainfed staple cropland under the high-budget scenario. Expansion is concentrated in tropical and subtropical regions, notably the Amazon basin, Central Africa, and Southeast Asia, where young forest and shrubland often offer the largest expansion areas. Herbaceous and barren classes appear more locally and at a smaller total area. Most grid cells remain unconverted; only parcels selected by the global budget allocation are shown. Where multiple expansion land-cover types are rainfed in the same cell, the map displays the class with the largest rainfed expansion area in that cell for visual clarity. Legend values report total selected area (Mha) by displayed class. Saline-groundwater zones (shaded) remain rainfed-only throughout. Together with the cropland-upgrade maps, this figure shows that expansion at rainfed intensity is geographically distinct from irrigation upgrades on existing cropland.

Figure 6 shows where the optimal allocation expands onto non-cropland, classified by the land cover that is converted rather than by post-conversion management. Across the ~\$8.9T / 2.8 Gt yr^{-1} allocation, selected expansion totals about 409 Mha: roughly 71 Mha from herbaceous vegetation, 153 Mha from shrubs, 66 Mha from barren land, and 119 Mha from young forest. Young-forest conversion is concentrated in the Amazon and parts of Southeast Asia; shrub and barren expansion are more prominent in Australia, parts of Africa, and South Asia; herbaceous expansion is more scattered, including temperate and subtropical fringes. Unlike the rainfed-only expansion map, irrigated conversion is included here, so regions such as interior Australia appear where expansion is largely irrigated. Saline-groundwater zones (shaded) can still host rainfed expansion but not new irrigation.

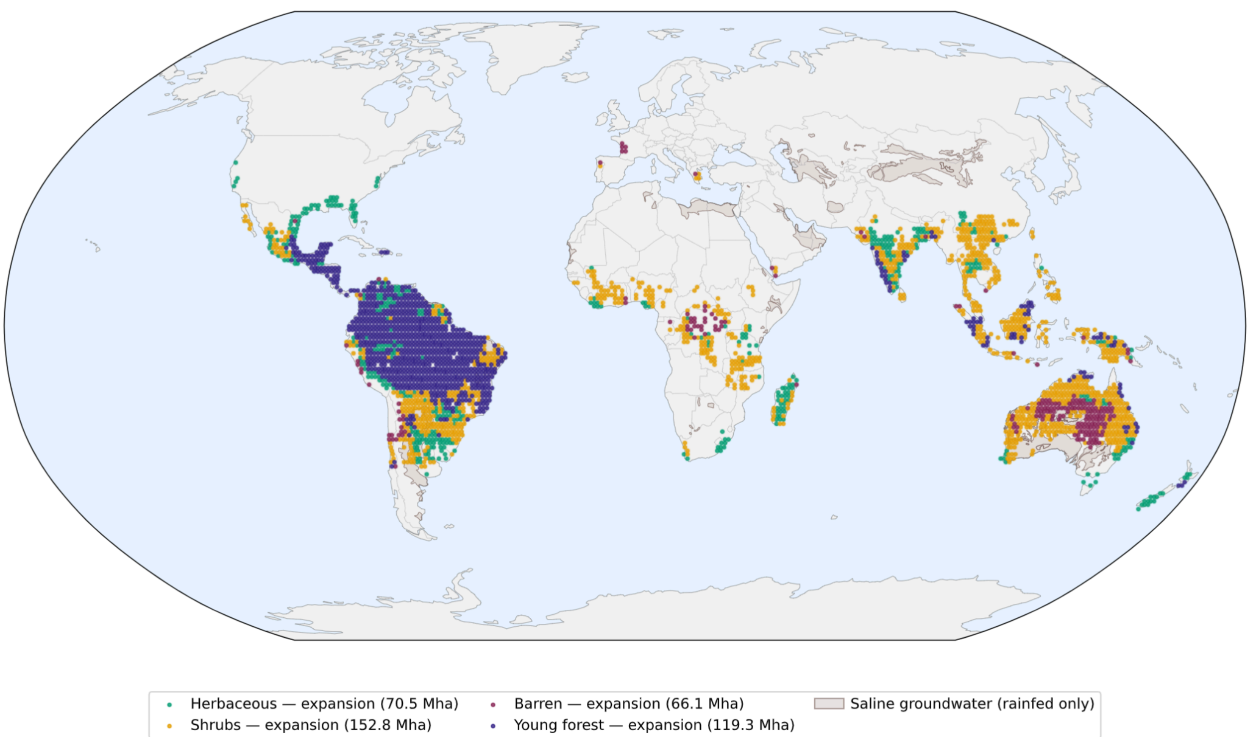

Figure 6. Agricultural expansion onto non-cropland in the optimal allocation, coloured by pre-expansion land cover (herbaceous, shrubs, barren, and young forest). Markers show where expansion is selected whether the land is managed rainfed or with new irrigation; irrigation intensity is not shown (see Figure 5). Legend values are total selected expansion area (Mha) by land-cover class. Gray shading marks saline-groundwater zones, where new irrigation is disallowed.

3.3 Global and Per-Country Supply Curves

Figure 7 shows the marginal cost of additional food production as cumulative investments expand. The solid line is the global supply curve, with the y-axis reporting marginal cost and the x-axis reporting cumulative production gain. The green shaded region indicates the portion of the curve financed under the selected budget, ending at $611 per tonne of dry carbohydrate equivalent and 2.80 Gt/yr dry carbohydrate equivalent. The upward slope indicates that the model first allocates lower-cost opportunities and then progressively moves to higher-cost sources as budget increases.

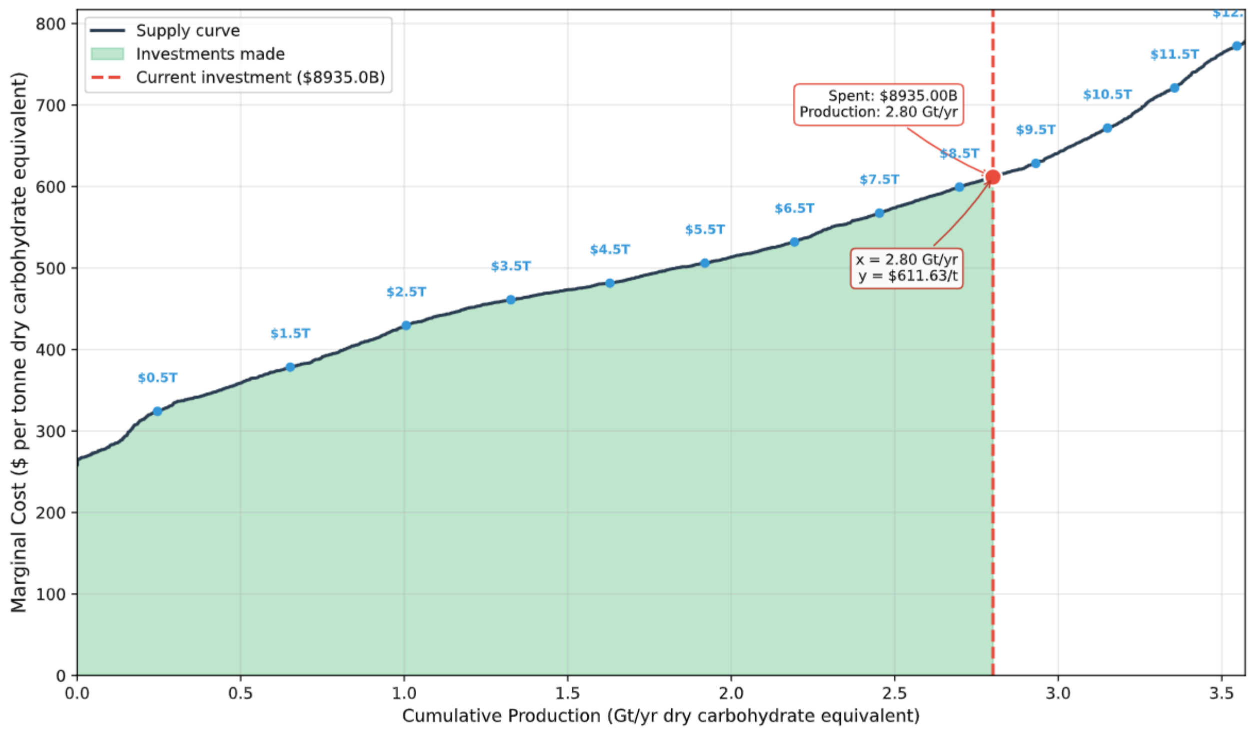

Figure 7. Global supply curve of staples (all land types) under the 150-Tg ASRS case (analysis years 2–8) for different investment budgets. Blue milestone markers label representative budget levels reached along the curve.

Figure 8 separates the global marginal-cost curve into current cropland (blue) and expansion (orange) contributions, with the dashed grey line showing the combined frontier when all sources are ordered by cost. Current cropland opportunities begin at low cost (annotated start near $258/t) but are exhausted earlier, after which marginal costs rise sharply. Expansion contributes much larger total potential at more gradually increasing marginal costs, with a steep tail at the highest-cost end.

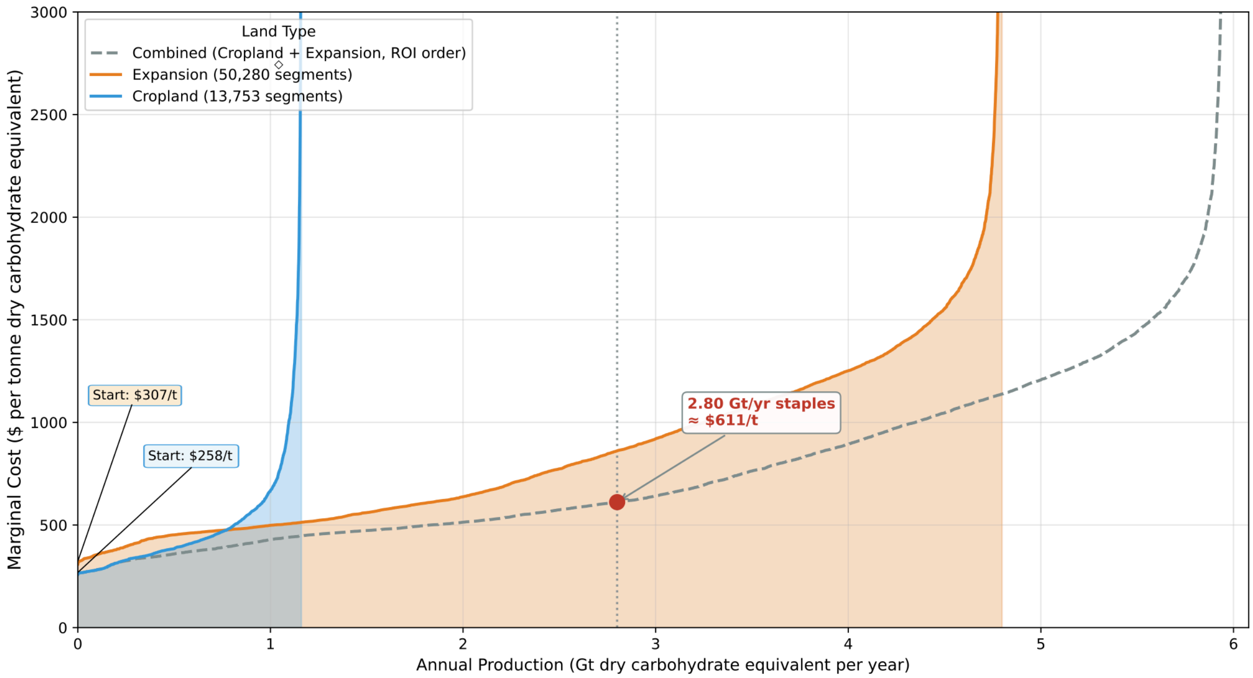

Figure 8. Global supply curves by land type under the 150-Tg ASRS case for analysis years 2–8, shown separately for current cropland only, expansion land only, and both current cropland and expanded land, across a range of investment budgets.

Figure C4 (Appendix C) shows the supply curve for the largest-producing countries, Australia and Brazil.

3.4 People Fed by Year

Figure 9 converts annual production to an equivalent "people fed" using a caloric conversion (2,100 kcal d^{-1} with a food-loss adjustment). These equivalents can exceed today's world population because the optimization maximizes staple caloric production for a given budget, rather than matching projected human food demand. Ambitious production targets are motivated in part by the fact that, outside the model, large shares of crop output normally go to animal feed and biofuels; those uses are not represented here. Production and people-fed equivalents rise over years 2–8 as farmers gain experience with new crops and locations and as ASRS conditions gradually improve. In later years of the shock, production could exceed direct-consumption needs, allowing stocks drawn down earlier to be rebuilt, after which additional area and irrigation effort would begin to decline.

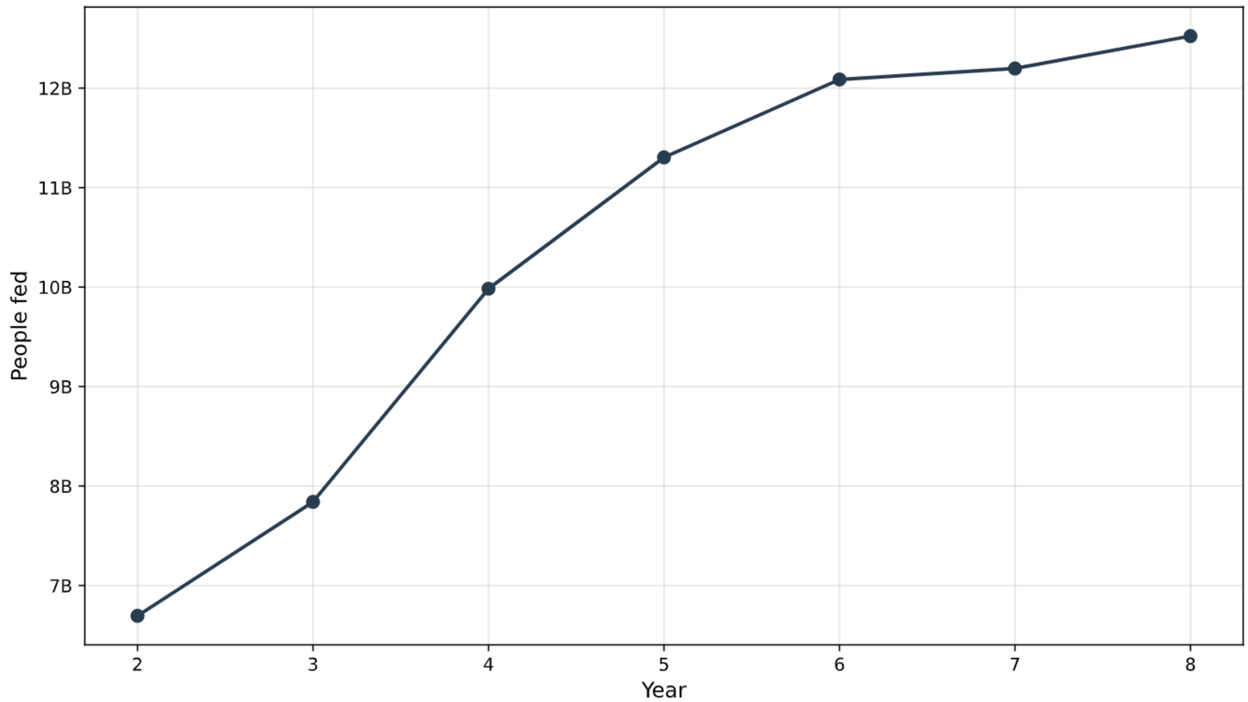

Figure 9. People fed by year from staple production in the 150-Tg ASRS case for analysis years 2–8, allowing investment on both existing cropland and newly expanded land, with a total investment budget of $8.935 trillion.

The global supply curve ranks investment segments by return on extra calories per extra dollar. Figure C5 (a) (Appendix C) contrasts the marginal cost of all segments taken in that global order (gray dashed curve) with the curve restricted to new pivot irrigation (orange). At the 2.8 Gt yr^{-1} dry carbohydrate point on the combined frontier, the marginal cost is \$611 t^{-1} dry carbohydrate equivalent; at that same marginal-cost level, only ~1.01 Gt yr^{-1} of the incremental staple supply is attributable to new pivot irrigation rather than to other management moves (e.g. rainfed expansion or continued legacy irrigation) that also enter the global ranking. Figure C5(b) (Appendix C) maps those economics onto groundwater depth: orange points are segments that lie on the new irrigation frontier at cumulative new-irrigation production $\leq$1.01 Gt yr^{-1} (the "reference" slice tied to the 2.8 Gt yr^{-1} / US\$611 t^{-1} point in panel a); gray points are other irrigation segments, which tend to sit at higher marginal cost for the same depth class. For the reference slice, median |WTD| is ~20 m and the mean ~24 m (vertical guides), with most mass at shallow depths in the inset histogram, consistent with cheap lift dominating the low-cost part of the irrigation queue while deeper water tables associate with more expensive marginal tonnes. Panel b also shows the distribution of well depths in gray and orange dots.

3.5 Sensitivity Analysis

Sensitivity is shown in Table 2. Generally the directions of changes are intuitive. However, one might not expect a greater cost of farming per hectare to result in more expansion. This is because the optimiser shifts toward higher-yield options to spread the fixed per-hectare farming costs over more production, and this means abandoning more low-yield currently cultivated land in favor of higher yield expanded land. Doubling any individual operation-and-maintenance, well, or pumping cost parameter in isolation affects the budget required to achieve the production goal by no more than approximately 2%.

Table 2. Sensitivity of the least-cost portfolio to individual cost parameters at a production target of 2.8 Gt yr^{-1} dry carbohydrate equivalent. Each row perturbs one parameter relative to the baseline cost scenario while holding all others fixed; the optimiser is re-run to meet the same production target. Values are for doubling the parameter unless noted.

Parameter (perturbation)	Δ budget (US$T; %)	Δ irrigated area (Mha; %)	Δ land expansion (Mha; %)
Farming variable cost per tonne per year (2× baseline)	+3.95; +44%	~0; ~0%	~0; ~0%
Farming base cost per hectare per year (2× baseline)	+1.90; +21%	+44; +14%	−13; −3%
Land expansion cost per hectare (joint min: $1,000 ha^{-1} herbaceous/shrub/barren; $3,000 ha^{-1} young forest)	−1.05; −12%	−69; −22%	+63; +14%
Land expansion cost per hectare (joint max: $6,000 ha^{-1} herbaceous/shrub/barren; $18,000 ha^{-1} young forest)	+1.99; +22%	+101; +32%	−40; −9%
Centre-pivot capital cost per hectare (2× baseline)	+0.53; +6%	−65; −20%	+57; +13%
Capital cost rate on irrigation CAPEX (2× baseline)	+0.29; +3%	−36; −11%	+29; +7%
Assumed depth below water table (pump/drill) (20 m → 6 m)	−0.16; −2%	+15; +5%	−10; −2%

Table 3 splits that scenario across five land-management pathways (new pivot irrigation on current cropland, rainfed current cropland, irrigated and rainfed expansion, and continued legacy irrigation). Most calories and areas sit in expansion rainfed and expansion irrigation, while pivot-irrigated hectares are concentrated in expansion irrigation, new irrigation on current cropland, and legacy irrigation; companion summary statistics give budget, average and marginal cost per tonne, people fed, and drilling time for the same crossing.

Table 3. Pathway allocation of modelled staple dry-carbohydrate production at ~2.8 Gt yr^{-1} (area, pivot irrigation, calorie and area shares, yields, pivot-weighted irrigation depths). I* indicates all irrigation capacities.

Pathway	Area (Mha)	Pivot-irrigated area (Mha)	% kcal	% area	t dry carb ha^{-1} yr^{-1}	t (pivot $ha)^{-1}$ yr^{-1}	Design average mm d^{-1}	Applied mm yr^{-1}
New irrigation on current cropland (I*, RI*)	63.4	49.7	8.06	8.58	3.56	4.11	2.21	127.4
Current rainfed (staple cropland, R)	178.1	0	16.39	24.12	2.58	—	—	—
Expansion irrigation (I*, RI*)	208.2	163.5	37.84	28.21	5.09	5.93	2.90	180.0
Expansion rainfed (R)	200.5	0	27.91	27.16	3.90	—	—	—
Current irrigated (legacy area, continue C)	88.0	88.0	9.80	11.92	3.12	3.12	4.0	142.8

4 Discussion

Across the scenarios examined, groundwater-based irrigation investment yields a substantial food-security payoff under severe ASRS conditions (150-Tg soot)relative to relying on rainfall alone after expansion is considered, though with strongly diminishing returns as the investment budget rises. By building directly on Mink-DSSAT simulations, the model captures complex interactions among temperature, precipitation, solar radiation, and crop physiology. This extends previous cropland expansion analyses (Monteiro et al., 2024) by incorporating irrigation costs alongside production estimates.

Economic modelling suggests that under the 150-Tg scenario, modelled investment-enabled production reaching 2.8 Gt/yr dry carbohydrate equivalent corresponds to an average cost of approximately $456/t (total cost divided by 19.6 Gt cumulative production), with a final marginal cost of $611/t at that scale. This compares with a present-day cost of $240–290/t dry carbohydrate equivalent for a commodity such as wheat (Agriculture and Horticulture Development Board, 2024; Brown et al., 2025; Oklahoma State University Extension, 2024). In reality, input prices would likely rise further during an ASRS, increasing costs beyond those modelled here. Supply in the early years, when food scarcity is most acute, would be lower and prices higher; this can be partially mitigated through stored food and rapidly scalable resilient foods (García Martínez et al., 2025; Rivers et al., 2024).

At the $8.935 T budget that delivers 2.8 Gt yr^{-1} dry carbohydrate, the marginal cost is about $611/t dry at the farm gate over a 7-year amortization. For comparison, methane single-cell protein under catastrophe-relevant assumptions (García Martínez et al., 2022, Table 7: 6-year plant lifetime and 24/7 construction) has a wholesale cost of $1,510–$2,580/t dry SCP, or about $3,020–$5,160/t after their 100% retail markup for distribution. Irrigated staple carbohydrate is substantially cheaper on a dry-mass basis, though the figures are not fully like-for-like: ours omit post-harvest processing and distribution, whereas SCP wholesale already embeds industrial production of a finished dry product, and the two commodities also differ in protein content.

Hydrogen-based single-cell protein is modelled at similarly high or higher wholesale costs (Martínez et al., 2021). The volume of food produced through expansion and irrigation also substantially exceeds that of other resilient-food options and involves more familiar crop types.

To assess the contribution of expanded irrigation capacity specifically, three paired comparisons are presented (staples, years 2–8; people-fed figures are annual averages of seven-year calculations using 2,100 kcal/day with a 29% food-loss adjustment). First, at a fixed budget of approximately $8.935 trillion, adding new centre-pivot irrigation on currently rainfed areas and on newly expanded cultivated land while continuing legacy irrigation supports food production equivalent to 1.0 billion additional people per year than a reallocation of the same budget relying solely on rainfed expansion and continuation of existing irrigation. Second, at a fixed production target of approximately 2.8 Gt/yr dry carbohydrate equivalent, achieving that target without new irrigation requires an additional $1.9 trillion, roughly 21% more than the cost when new irrigation is available. Third, the yield improvement attributable to first-time irrigation on parcels selected in the optimal solution translates to approximately 2.8 billion additional people equivalents per year in years 2 through 8, capturing only the irrigation-induced yield gain on those parcels and excluding both the calories produced through rainfed expansion and the contribution of legacy irrigated areas.

This cost ordering is robust to the land-preparation cost sensitivities reported here and to regional supply curves where shown: upgrading existing rainfed cropland is generally the cheapest source of additional calories, while expansion onto non-cropland is more costly but becomes increasingly important as budgets rise and low-cost opportunities are exhausted.

5 Limitations

Several limitations qualify how these results should be interpreted, as summarised in Table 4, which categorises key modelling choices as optimistic, pessimistic/conservative, or mixed with respect to food cost and production.

Table 4. Optimistic versus pessimistic assumptions regarding food cost and/or production.

Direction	Assumption / omission	Why it tilts that way
Pessimistic	Aquifer-based wells with a static water-table depth: wells 20 m deeper than the water table will likely be more than sufficient to accommodate 7 years of drawdown	Average water application over 7 years is 1.2 m and typical specific yield is 20% (Lohman, 1972, p. 8), producing 6 m drawdown if no recharge.
Pessimistic	Only diesel pumping assumed	Pumping costs may be lower because some will be electric instead of diesel
Optimistic	Existing irrigation infrastructure remains usable	Post-catastrophe repair and fuel/parts could be worse.
Pessimistic	No surface-water irrigation (canals, reservoirs, river diversions)	Omits a major class of potentially cheaper or larger-scale water delivery; food potential and $/calorie could improve if surface water were included.
Optimistic	Maximizing calories with staple crop switching	Ignores market preference
Pessimistic	No adaptation of non-staple crops	Non staple crop relocation would increase food production
Optimistic	Fixed cost/performance parameters (wells, pivots, drilling speeds, $/m pumping)	Actual material and labour prices post-ASRS could be much higher.
Pessimistic	Current food waste continues	Higher prices would reduce food waste
Pessimistic	Climate data uses existing crops for transpiration	Relocated crops and irrigation would cause greater transpiration, increasing precipitation, increasing yields.
Optimistic	Modelled yields do not capture all possible failure modes, such as wheat stem lodging under nuclear-winter irradiance	Growth-chamber experiments simulating 150 Tg conditions in South Australia found wheat stems collapsed under their own weight, something DSSAT does not account for (Blouin et al., 2026).
Optimistic	Fertilizer and pesticide application rates per ha per year continue	This would require scale up of fertilizer and pesticide production if there is major infrastructure destruction.

Direction	Assumption / omission	Why it tilts that way
Optimistic	Planting month is optimised for each year	The best planting month is chosen for each year of catastrophe, which changes as the climate improves. This is optimistic compared to using the same month every year, but it is pessimistic compared to planting in the optimal week each year.
Optimistic	Inexperience factors in the first 3 years of the catastrophe	Yields are lower to account for farmers' inexperience with new crops and for the effects of planting in a newly converted area.
Pessimistic	Expansion limited to herbaceous vegetation, barren land, shrubland, and young forest	Expansion is limited to the land types that would be the easiest to clear, but excludes areas that could also be used for crop production such as older forest.
Optimistic	Some soil characteristics are not considered	Soil nitrogen and the physical properties of the soil are considered, but pH and other biological and chemical characteristics are not, which can lower yields.
Pessimistic	Current population assumed	The catastrophe would result in fewer people who have to be fed.
Optimistic	Global food trade is maintained	Geopolitical tensions could lead to some nations being unwilling to export their food in a catastrophe
Optimistic	The model does not represent groundwater depletion over time. Each grid cell is assigned a fixed water-table depth, and well costs, pumping, and drilling effort are scaled from that static snapshot.	As extraction proceeds, real water tables would drop further than the static value used, raising pumping cost and drilling depth requirements over the modelled horizon; the model does not capture this feedback, so the model likely underestimates costs in the later years for cells where groundwater is being used up.

The model does not yet incorporate fertiliser or pesticide supply chains, regulatory constraints, or their costs, all of which could materially affect feasibility when irrigation expands area or intensity. In particular, animal and sterilised human waste as fertiliser sources have not been analysed.

Under the assumed drilling fleet, 213 Mha of newly irrigated centre-pivot footprint requires approximately 45 days of sequential drilling for the staples pathway alone; in practice, more drilling capacity would be needed for non-staple crops. The drilling constraint and the land-clearance ceiling from Monteiro et al. (2024) are used as consistency checks but are not fully co-optimised within the model.

6 Conclusions

This study demonstrates that optimised irrigation investment can make a large, practical contribution to food security under a severe 150 Tg nuclear-winter scenario. In the global supply curve, marginal cost reaches approximately $611/t dry carbohydrate equivalent at roughly 2.8 Gt/yr, and total modelled production at that scale is equivalent to feeding on the order of 10 billion people per year over the analysis window (including rainfed and pre-existing irrigated cropland, not only calories from new irrigation).

The cost ordering is clear and robust: the cheapest calories come from cultivating existing cropland rainfed and continuing to operate legacy irrigated cropland, and new pivot irrigation enters only once those options are largely exhausted. Among new irrigation investments, upgrading existing rainfed cropland is cheaper than irrigating newly expanded land, but the eligible area is small, so expansion onto previously uncultivated land supplies most of the additional production as budgets rise and cheaper opportunities run out. New irrigation contributes approximately 1.0 billion additional people equivalents per year under a fixed budget, reduces the cost of meeting a fixed production target by approximately 18%, and delivers approximately 2.8 billion people-equivalents per year in direct yield gain on newly irrigated parcels.

7 Future Work

Future work should extend the analysis to milder scenarios with soot injection below 150 Tg to characterise how irrigation cost-effectiveness, optimal regional allocation, and the global supply curve shift across the full spectrum of plausible catastrophe magnitudes.

A fully autarkic scenario, in which the optimisation is rerun within national borders with no cross-border trade assumed, is beyond the scope of the present study but represents a worthwhile direction for future research, given that political constraints may significantly affect trade flows during a catastrophe.

Another priority for future work also is to extend the optimisation beyond staple crops to non-staple crops, which would raise both calorie and nutrient supply but also increase land, water, capital, and drilling requirements relative to the staples-only pathway modelled here.

Further priorities include: testing robustness under no-trade and regionalised constraints; adding basin-scale hydrology and surface-water options; integrating fertiliser requirements (fertiliser and pesticide rates, availability, transport, pricing, and environmental safeguards) alongside irrigation investment; and co-optimising irrigation with other resilient-food interventions (including seaweed, greenhouses, microbial protein, and lignocellulosic sugar) within a unified decision framework.

8 Credit authorship contribution statement

Pinkeshkumar Attarwala: Conceptualisation, Methodology, Software, Formal analysis, Investigation, Data curation, Writing –original draft, Writing – review and editing, Visualisation. Simon Blouin: Methodology, Software, Formal analysis, Writing – review and editing. Mike Hinge: Conceptualisation, Methodology, Writing – review and editing. Luisa Lopes Monteiro: Data curation. Mohammadreza Ebrahimnataj Tiji: Writing – review and editing. Thomas Cochrane: Supervision, Writing – review and editing. David Denkenberger: Conceptualisation, Methodology, Supervision, Funding acquisition, Writing – review and editing.

9 Declaration of competing interest

The authors declare that they have no known competing financial interests or personal relationships that could have appeared to influence the work reported in this paper.

10 Funding

This work was supported by the Alliance to Feed the Earth in Disasters (ALLFED). The funders had no role in the study design, data collection and analysis, decision to publish, or preparation of the manuscript. It was also supported by the Department of Mechanical Engineering at the University of Canterbury Scholarship.

11 Acknowledgements

The authors thank colleagues at the Alliance to Feed the Earth in Disasters (ALLFED) and the University of Canterbury for helpful discussions and feedback on earlier drafts.

12 Declaration of generative AI and AI-assisted technologies in the writing process

During the preparation of this work, the authors used ChatGPT solely to improve the grammar and language of the manuscript. After using this tool, the authors reviewed and edited the content as needed and take full responsibility for the content of the publication.

References

Agriculture and Horticulture Development Board. (2024, March 27). *How do UK wheat overhead costs stack up internationally: Grain market daily*. https://ahdb.org.uk/news/how-do-uk-wheat-overhead-costs-stack-up-internationally-grain-market-daily

Alvarado, K. A., Mill, A., Pearce, J. M., Vocaet, A., & Denkenberger, D. (2020). Scaling of greenhouse crop production in low sunlight scenarios. *Science of the Total Environment*, *707*, 136012. https://doi.org/10.1016/j.scitotenv.2019.136012

Al-Ghobari, H., & Dewidar, A. Z. (2021). A comparative study of standard center pivot and growers-based modified center pivot for evaluating uniformity coefficient and water distribution. *Agronomy*, *11*(8), 1675. https://doi.org/10.3390/agronomy11081675

Ballard, T. E. (2017, September 27). *Well entrance velocity: An often overlooked well performance factor*. Southeast Hydrogeology. https://sehydrogeology.com/well-entrance-velocity-often-overlooked-well-performance-factor/

Blouin, S., Rivers, M., Hinge, M., Antonietta, M., Jimenez, I., Jehn, F. U., & Denkenberger, D. C. (2025). *Strategic crop relocation could substantially mitigate nuclear winter yield losses* [Preprint]. EarthArXiv. https://doi.org/10.31223/X5GN09

Blouin, S., Abrams, D. R., Ben-Zeev, R., Anderson, C. T., Lasky, J. R., & Denkenberger, D. (2026). *Crop yields under simulated nuclear winter: A growth chamber experiment* [Preprint]. bioRxiv. https://doi.org/10.64898/2026.05.05.723012

BrasilAgro–Companhia Brasileira de Propriedades Agrícolas. (2014). *Annual report (Form 20-F) for the fiscal year ended June 30, 2014*. U.S. Securities and Exchange Commission. https://www.sec.gov/Archives/edgar/data/1499849/000119312514391641/d810767d20f.htm

Brown, B., Kientzy, D., Bish, M., Nelson, K., & Bradley, K. (2025). Winter wheat planning budget (Publication G656; revised October 2025). University of Missouri Extension. https://extension.missouri.edu/publications/g656

Business Research Company. (2026). *Rotary drilling rig global market report*. https://www.thebusinessresearchcompany.com/report/rotary-drilling-rig-global-market-report

Cascade Environmental. (2020, September 8). *Common questions about rotary drilling, Part 2*. https://www.cascade-env.com/resources/blogs/common-questions-about-rotary-drilling-part-2/

Castillo, J. G., & Zhangallimbay, D. (2022). The social discount rate in the evaluation of investment projects: An application for Ecuador. *CEPAL Review*, *2021*(134), 75–95. https://doi.org/10.18356/16840348-2021-134-4

Coupe, J., Bardeen, C. G., Robock, A., & Toon, O. B. (2019). Nuclear winter responses to nuclear war between the United States and Russia in the Whole Atmosphere Community Climate Model Version 4 and the Goddard Institute for Space Studies ModelE. *Journal of Geophysical Research: Atmospheres*, *124*(15), 8522–8543. https://doi.org/10.1029/2019JD030509

CVFPB. (2020). *EIS Attachment 8b: Well drilling costs* [PDF]. State of California. https://cvfpb.ca.gov/wp-content/uploads/2020/11/8b.-EIS-Attachment-Well-Drilling-Costs.pdf

DataIntelo. (2026). *Water well drilling rig market*. https://dataintelo.com/report/water-well-drilling-rig-market

Department of Employment, Economic Development and Innovation. (2011). Centre pivot/lateral move irrigation: Overview. Queensland Government. https://moreprofitperdrop.wordpress.com/wp-content/uploads/2011/11/cplm.pdf

Elliott, J., Deryng, D., Müller, C., Frieler, K., Konzmann, M., Gerten, D., ... & Wisser, D. (2014). Constraints and potentials of future irrigation water availability on agricultural production under climate change. *Proceedings of the National Academy of Sciences*, *111*(9), 3239–3244.

Feili Pump. (2026). At what depth should a submersible pump be installed? Retrieved August 3, 2026, from https://www.cttpump.com/at-what-depth-should-a-submersible-pump-be-installed/

Fist, T., Adesanya, A. A., Denkenberger, D., & Pearce, J. M. (2021). Global distribution of forest classes and leaf biomass for use as alternative foods to minimize malnutrition. *World Food Policy*, *7*(2), 128–146.

Food and Agriculture Organization of the United Nations. (1985). *Water quality for agriculture* (Irrigation and Drainage Paper 29 Rev. 1).

Food and Agriculture Organization of the United Nations. (2011). *The state of the world's land and water resources for food and agriculture: Managing systems at risk*.

Food and Agriculture Organization of the United Nations. (2019). *The state of food and agriculture 2019: Moving forward on food loss and waste reduction*. https://www.fao.org/3/ca6030en/ca6030en.pdf

Food and Agriculture Organization of the United Nations (FAO). (2026). FAOSTAT: Food Balances. Rome, Italy: FAO. Retrieved August 14, 2026, from https://www.fao.org/faostat/en/#data/FBS

Frenken, K. (Ed.). (2012). *Irrigation in Southern and Eastern Asia in figures: AQUASTAT survey 2011* (FAO Water Reports No. 37). Food and Agriculture Organization of the United Nations.

García Martínez, J. B., Behr, J., Pearce, J., & Denkenberger, D. (2025). Resilient foods for preventing global famine: A review of food supply interventions for global catastrophic food shocks including nuclear winter and infrastructure collapse. *Critical Reviews in Food Science and Nutrition*, *65*(2), 1–27. https://doi.org/10.1080/10408398.2024.2431207

García Martínez, J. B., Pearce, J. M., Throup, J., Cates, J., Lackner, M., & Denkenberger, D. C. (2022). Methane single cell protein: potential to secure a global protein supply against catastrophic food shocks. *Frontiers in Bioengineering and Biotechnology, 10*, 906704

Global Growth Insights. (2026). *Water well drilling market report* (Report No. 115113). https://www.globalgrowthinsights.com/market-reports/water-well-drilling-115113

GlobalPetrolPrices.com. (2026). *Diesel prices, liter*. Retrieved April 27, 2026, from https://www.globalpetrolprices.com/diesel_prices/

Gustavsson, J., Cederberg, C., Sonesson, U., van Otterdijk, R., & Meybeck, A. (2011). *Global food losses and food waste: Extent, causes and prevention*. Food and Agriculture Organization of the United Nations. https://www.fao.org/3/i2697e/i2697e.pdf

Hassani, A., Azapagic, A., & Shokri, N. (2020). Predicting long-term dynamics of soil salinity and sodicity on a global scale. *Proceedings of the National Academy of Sciences*, *117*(52), 33017–33027. https://doi.org/10.1073/pnas.2013771117

Hinge, M., Gajewski, Ł. G., Frank, R., Blouin, S., Jehn, F. U., & Denkenberger, D. (2026). *Calculating equilibrium cereal prices during a multi-year productivity shock. Available at SSRN 6298706.*

Industry Research. (2026). *Water well drilling rigs market* (Report No. 105294). https://www.industryresearch.biz/market-reports/water-well-drilling-rigs-market-105294

Hunter Agricultural Irrigation. (2023, May 12). *Optimize your center pivot irrigation water use with pressure regulators*. https://agriculture.hunterirrigation.com/news/2023/05/12/optimize-your-center-pivot-irrigation-water-use-pressure-regulators

Intergovernmental Panel on Climate Change. (2019). *2019 refinement to the 2006 IPCC guidelines for national greenhouse gas inventories* (E. Calvo Buendia, K. Tanabe, A. Kranjc, J. Baasansuren, M. Fukuda, S. Ngarize, A. Osako, Y. Pyrozhenko, P. Shermanau, & S. Federici, Eds.; Vol. 2: Energy). IPCC. https://www.ipcc-nggip.iges.or.jp/public/2019rf/

Intergovernmental Panel on Climate Change. (2022). *Climate change 2022: Impacts, adaptation and vulnerability: Contribution of Working Group II to the Sixth Assessment Report of the Intergovernmental Panel on Climate Change*. Cambridge University Press.

International Energy Agency. (2024). *Oil 2024: Analysis and forecast to 2030*. https://www.iea.org/reports/oil-2024

Jägermeyr, J., Gerten, D., Schaphoff, S., Heinke, J., Lucht, W., & Rockström, J. (2016). Integrated crop water management might sustainably halve the global food gap. *Environmental Research Letters*, *11*, 025002. https://doi.org/10.1088/1748-9326/11/2/025002

Jägermeyr, J., Robock, A., Elliott, J., Müller, C., Xia, L., Khabarov, N., Folberth, C., Schmid, E., Liu, W., Zabel, F., Rabin, S. S., Puma, M. J., Heslin, A. C., Franke, J., Foster, I., Asseng, S., Bardeen, C. G., Toon, O. B., & Rosenzweig, C. (2020). A regional nuclear conflict would compromise global food security. *Proceedings of the National Academy of Sciences, 117*(13), 7071–7081. https://doi.org/10.1073/pnas.1919049117

Jehn, F. U., Dingal, F. J., Mill, A., Harrison, C., Ilin, E., Roleda, M. Y., James, S. C., & Denkenberger, D. (2024). Seaweed as a resilient food solution after a nuclear war. *Earth's Future*, *12*(1), e2023EF003710. https://doi.org/10.1029/2023EF003710

Lamm, F. R., & Trooien, T. P. (2003). Subsurface drip irrigation for corn production: A review of 10 years of research in Kansas. *Irrigation Science*, 22(3-4), 195–200. https://doi.org/10.1007/s00271-003-0085-3

Lohman, S. W., 1972, Ground-Water Hydraulics: U.S. Geological Survey Professional Paper 708, 70 p., https://doi.org/10.3133/pp708.

Martínez, J. B. G., Egbejimba, J., Throup, J., Matassa, S., Pearce, J. M., & Denkenberger, D. C. (2021). Potential of microbial protein from hydrogen for preventing mass starvation in catastrophic scenarios. *Sustainable Production and Consumption*, *25*, 234–247.

Michigan State University Extension. (2010). 160-acre center pivot. https://www.canr.msu.edu/irrigation/Irrigation-Planning/Irrigation-Costs-Pages/160-acre-center-pivot

Mora, M., Vera, J., Rocamora, C., & Abadia, R. (2013). Energy efficiency and maintenance costs of pumping systems for groundwater extraction. Water Resources Management, 27, 4395–4408. https://doi.org/10.1007/s11269-013-0423-z

Monteiro, L. L., Hinge, M., Blouin, S., Rivers, M., van der Walt, J. D., & Denkenberger, D. (2024). *Expansion of cropland area during an abrupt sunlight reduction scenario* [Preprint]. EarthArXiv. https://doi.org/10.31223/X5MQ54

Oklahoma State University Extension. (2024). *Conventional tillage wheat budget (2024)*. https://extension.okstate.edu/programs/farm-management-and-finance/budgets/sample-budgets/site-files/docs/2024/conventional-tillage-wheat-2024-a.pdf

Planète Énergies. (2026). *Life cycle of oil and gas fields*. https://www.planete-energies.com/en/media/article/life-cycle-oil-and-gas-fields

Poulter, B., Aragão, L., Andela, N., Bellassen, V., Ciais, P., Kato, T., Lin, X., Nachin, B., Luyssaert, S., Pederson, N., Peylin, P., Piao, S., Pugh, T., Saatchi, S., Schepaschenko, D., Schelhaas, M., & Shivdenko, A. (2019). *The global forest age dataset and its uncertainties (GFADv1.1)* [Data set]. NASA National Aeronautics and Space Administration; PANGAEA. https://doi.org/10.1594/PANGAEA.897392

Queensland Department of Employment, Economic Development and Innovation. (2011). *Centre pivot/lateral move irrigation*. https://moreprofitperdrop.wordpress.com/wp-content/uploads/2011/11/cplm.pdf

Rivers, M., Hinge, M., Rassool, K., Blouin, S., Jehn, F. U., García Martínez, J. B., Grilo, V. A., Jaeck, V., Tieman, R. J., Mulhall, J., Butt, T. E., & Denkenberger, D. C. (2024). Food system adaptation and maintaining trade could mitigate global famine in abrupt sunlight reduction scenarios. *Global Food Security*, *43*, 100807. https://doi.org/10.1016/j.gfs.2024.100807

Robock, A. (2010). Nuclear winter. *Wiley Interdisciplinary Reviews: Climate Change*, *1*(3), 418–427.

Robertson, R. D. (2017). *Mink: Details of a global gridded crop modeling system*. International Food Policy Research Institute (IFPRI). https://hdl.handle.net/10568/148024

Rosa, L. (2022). Adapting agriculture to climate change via sustainable irrigation: Biophysical potentials and feedbacks. *Environmental Research Letters*, *17*, 063008. https://doi.org/10.1088/1748-9326/ac7408

Rosa, L., Chiarelli, D. D., Sangiorgio, M., Beltran-Peña, A. A., Rulli, M. C., D'Odorico, P., & Fung, I. (2020). Potential for sustainable irrigation expansion in a 3 °C warmer climate. *Proceedings of the National Academy of Sciences*, *117*(47), 29526–29534. https://doi.org/10.1073/pnas.2017796117

Smith, P. (2015). Is your diesel pump costing you money? Primefact 1425 (1st ed.). NSW Department of Primary Industries. https://www.dpird.nsw.gov.au/__data/assets/pdf_file/0004/165217/is-your-diesel-pump-costing-you-money.pdf

Throup, J., García Martínez, J. B., Bals, B., Cates, J., Pearce, J. M., & Denkenberger, D. C. (2022). Rapid repurposing of pulp and paper mills, biorefineries, and breweries for lignocellulosic sugar production in global food catastrophes. *Food and Bioproducts Processing*, *131*, 22–39. https://doi.org/10.1016/j.fbp.2021.10.012

Tidal Petroleum. (2026). *Drilling cost*. Retrieved May 14, 2026, from https://www.tidalpetroleum.com/processes/drilling-cost

Tuanmu, M.-N., & Jetz, W. (2014). A global 1-km consensus land-cover product for biodiversity and ecosystem modelling. *Global Ecology and Biogeography*, *23*(9), 1031–1045. https://doi.org/10.1111/geb.12182

Turnbull, R. (2026). Entrance velocity: Its importance to well design (Technical Memorandum 006-6). Roscoe Moss Company.

https://roscoemoss.com/wp-content/uploads/techmemos/TechMemo006-6-EntranceVelocity-ItsImportancetoWellDesign.pdf

UNESCO Intergovernmental Hydrological Programme. (2024). *Areas of saline groundwater* [Data set]. IHP Water Information Network System. https://ihp-wins.unesco.org/dataset/areas-of-saline-groundwater/resource/db8b3fd1-1b2a-460c-a2b9-fab4d83c9b64

United Nations Educational, Scientific and Cultural Organization–International Hydrological Programme. (2013). *IHP-WINS: Areas of saline groundwater* [Data set]. UNESCO-IHP. https://ihp-wins.unesco.org/dataset/areas-of-saline-groundwater

United Nations Environment Programme. (2021). *Food Waste Index Report 2021*. https://www.unep.org/resources/report/unep-food-waste-index-report-2021

U.S. Department of Agriculture, Economic Research Service. (2026). *Commodity costs and returns: Wheat* [WheatCostReturn.xlsx]. https://www.ers.usda.gov/data-products/commodity-costs-and-returns

Western Drilling. (2024, September 9). *All about water well diameter sizes*. Oklahoma Water Drilling. https://oklahomawaterdrilling.com/all-about-water-well-diameter-sizes/

Wilson, N., Payne, B., & Boyd, M. (2023). Mathematical optimization of frost resistant crop production to ensure food supply during a nuclear winter catastrophe. *Scientific Reports*, *13*, 8254. https://doi.org/10.1038/s41598-023-35354-7

World Bank. (2021). *International Comparison Program (ICP).* Retrieved July 28, 2026, from https://www.worldbank.org/en/programs/icp

Xia, L., Robock, A., Scherrer, K., Harrison, C. S., Bodirsky, B. L., Weindl, I., Jägermeyr, J., Bardeen, C. G., Toon, O. B., & Heneghan, R. (2022). Global food insecurity and famine from reduced crop, marine fishery and livestock production due to climate disruption from nuclear war soot injection. *Nature Food*, *3*(8), 586–596. https://doi.org/10.1038/s43016-022-00573-0

Yu, Q., You, L., Wood-Sichra, U., Ru, Y., Joglekar, A. K. B., Fritz, S., Xiong, W., Lu, M., Wu, W., & Yang, P. (2020). A cultivated planet in 2010 – Part 2: The global gridded agricultural-production maps. *Earth System Science Data*, *12*(4), 3545–3572. https://doi.org/10.5194/essd-12-3545-2020

Zhuang, J., Liang, Z., Lin, T., & de Guzman, F. D. (2007). *Theory and practice in the choice of social discount rate for cost–benefit analysis: A survey* (ADB Economics Working Paper Series No. 94). Asian Development Bank. https://www.adb.org/publications/theory-and-practice-choice-social-discount-rate-cost-benefit-analysis-survey

Appendix A. Irrigation Cost Model: Parameter Derivation

This appendix documents the derivation of each cost parameter used and assumptions made in Section 2.1.6. All parameters are drawn from published sources.

A1. Well capital cost (C_{wm})

Well capital cost is derived from the well-drilling cost schedules reported by the Central Valley Flood Protection Board (CVFPB, 2020) for an 8-inch-diameter (200 mm) well, which quote $84 per foot of depth for a complete water well system. Applying an inflation factor of 1.287 (Minneapolis Federal Reserve calculator, 2020 to 2026, USD) and converting to metric units yields $355 per metre of well depth.

A2. Centre pivot cost (C_{total})

Centre-pivot capital cost is derived from the Michigan State University Extension 160-acre centre-pivot costing example (MSU Extension, 2010), which reports a fully installed cost of $62,000 (2010 USD) for a standard 160-acre system with end gun irrigating 132 acres (53.4 ha), i.e. $1,161 per irrigated hectare. Applying an inflation factor of 1.53 (2010 to 2026, USD) yields C_{total} = $1,776 ha^{-1}. The Queensland Government centre-pivot overview (DEEDI, 2011), which reports AUD 2,500–5,500 ha^{-1} (USD 1,750–3,850 ha^{-1}) including pipework, pumping equipment, and the power plant, serves as an upper-bound cross-check: our pivot-only figure lies below this all-inclusive range, as it should. MSU Extension also reports annual pivot repair costs of approximately 3% of pivot capital, yielding the per-hectare irrigation maintenance figure C_{mi} = 0.03 × 1,776 = $53 ha^{-1} yr^{-1} (Section A4).

A3. Pumping costs (C_d, C_{fx}, C_{mv})

Depth-dependent pumping cost (C_d = 0.0015 USD m^{-3} m^{-1}) and fixed conveyance cost (C_{fx} = 0.0098 USD m^{-3}) are derived from diesel pump performance data reported by Smith (2015), using specific fuel consumption of 0.26 L kWh^{-1} (Water Pumping Institute, 2026), pump efficiency E_p = 0.70 (Foley, 2015), motor efficiency E_m = 0.90 (Foley, 2015), and generator efficiency E_g = 0.90 (Algrain, 2017), combined with a global average diesel price of \$1.22 L^{-1} averaged across all the countries globally (GlobalPetrolPrices.com, 2026). Above-ground distribution cost (C_{mv} = 0.0187 USD m^{-3}) reflects the pressure head required to operate centre pivot laterals, taken as 17.5 psi average (Hunter Agricultural Irrigation, 2023), converted to an equivalent hydraulic head of 12.3 m.

A4. Maintenance costs (C_{md}, C_{mp}, C_{mi})

Pump maintenance is based on Mora et al. (2013), who report the cost of a single maintenance intervention (crane extraction plus workshop refurbishment) for deep-well submersible pumps serving agricultural irrigation in Spain and estimate a service life of 8,000 operating hours between interventions. Evaluating their cost equation for a 200-mm pump and fitting a linear relation gives a per-event cost of $C_{md}\,d + C_{mp}$, with C_{md} = \$21.6 per event per metre of water-table depth and C_{mp} = \$2,488 per event, after conversion at 1.10 USD/EUR and adjustment to 2026 price levels using euro-area HICP inflation (factor 1.34). The per-event cost is annualised by the expected number of events per year. Operating hours follow directly from pumped volume and well capacity: a well pumping at Q_w = 1,579 m^3 day^{-1} delivers V_m = $(Q_w/24) \times 8{,}000 \approx 5.3 \times 10^5$ m^3 between interventions, so pump maintenance per hectare per year is $(C_{md}\,d + C_{mp})\,Q/V_m$, where Q is the pumped volume per hectare per year (Eq. 7). Implied operating hours in the model average 700–2,000 h yr^{-1} depending on irrigation capacity. Per-hectare irrigation maintenance C_{mi} = \$53 ha^{-1} yr^{-1} is 3% of pivot capital annually, following MSU Extension (2010) (Section A2).

A5. Well yield (Q_w) and pump depth offset (d_0)

Maximum well discharge is calculated from safe screen entrance velocity (0.46 m/s, Turnbull, 2026) and a nominal 8-inch diameter well (Western Drilling, 2024), allowing for the casing and the casing shoe, the corresponding standard diameter is 225 mm, giving Q_w = 1,579 m^3 day^{-1} per well. The pump depth offset (d_0 = 20 m (including the minimum requirement plus an assumed safety allowance)) represents the minimum recommended submersible pump installation depth below the water table (Feili Pump, 2026).

A6. Capital annualisation

CAPEX is annualised using the factor, (1/T) + r = (1/7) + 0.10 = 0.2429 yr^{-1}, where T = 7 years is the depreciation period and r = 0.10 is the cost of capital, consistent with World Bank and Asian Development Bank discount rates for comparable projects (Zhuang et al., 2007; Castillo & Zhangallimbay, 2022).

Appendix B. Drilling Rig Fleet Sizing

This appendix documents the derivation of the drilling rig fleet counts used in Section 2.2.4 to constrain the rate of new well installation. Three rig classes are considered: agricultural, oil and gas, and residential water-well drilling. Available fleet size for each class is estimated from global market value and average unit cost, following the relationship: annual production (units) equals global market value ($/yr) divided by average cost per rig (USD); total stock equals annual production multiplied by average service life (years).

B1. Oil and Gas Rig Stock

The global oil and gas rig count is taken directly from industry reporting rather than derived from market value, since active rig counts are tracked and published in real time. The total is 1,479 rigs (Savage, 2025), comprising the United States (539 rigs: 411 oil, 128 gas), Canada (180 rigs), Saudi Arabia (110 rigs), Russia (300 rigs), China (225 rigs), and other countries including the United Arab Emirates, Iraq, Brazil, and Norway (125 rigs combined).

B2. Water-well Drilling Rig Market

The total global water-well drilling rig market is valued at $552.28 million per year (Maia Research, 2026). This market is split between agricultural and residential end uses using a reported residential share of 62% of the global total (Industry Research, 2026; Maia Research, 2026), giving an agricultural market value of $209.87 million per year and a residential market value of $342.41 million per year.

B3. Agricultural rig stock

Average cost per agricultural drilling rig is estimated at $121,083, derived as the mean of three water-well drilling rig categories reported by RoadSky Corporation (2025): small portable rigs ($1,500–$10,000; midpoint $5,750), truck- and trailer-mounted rigs ($15,000–$100,000; midpoint $57,500), and heavy-duty rotary rigs ($100,000–$500,000; midpoint $300,000). Dividing the agricultural market value ($209.87 million per year) by this average unit cost gives an annual production of approximately 700 rigs per year. Applying an average operating life of 15 years (Planète Énergies, 2026) yields a total agricultural rig stock of approximately 10,500 units.

B4. Residential Rig Stock

Using the same average unit-cost basis ($121,083) and the residential market value of $342.41 million per year, annual residential rig production is approximately 2,828 units per year. Applying the same 15-year average service life (Planète Énergies, 2026) yields a total residential rig stock of approximately 42,400 units.

B5. Summary

The resulting fleet sizes used in the optimisation model (Section 2.2.4) are 10,493 agricultural well-drilling rigs, 1,479 oil and gas rigs, and 42,419 residential well-drilling rigs. Oil and gas rigs are included as a potential source of additional agricultural drilling capacity given their higher penetration rate (1,000 ft/day compared with 275 ft/day for agricultural and residential rigs), though cross-class reallocation would require conversion equipment and crew retraining not costed here. We assume 8 hr/day and 7 days operation days per week when calculating the number of wells.

Appendix C. Supplementary Figures

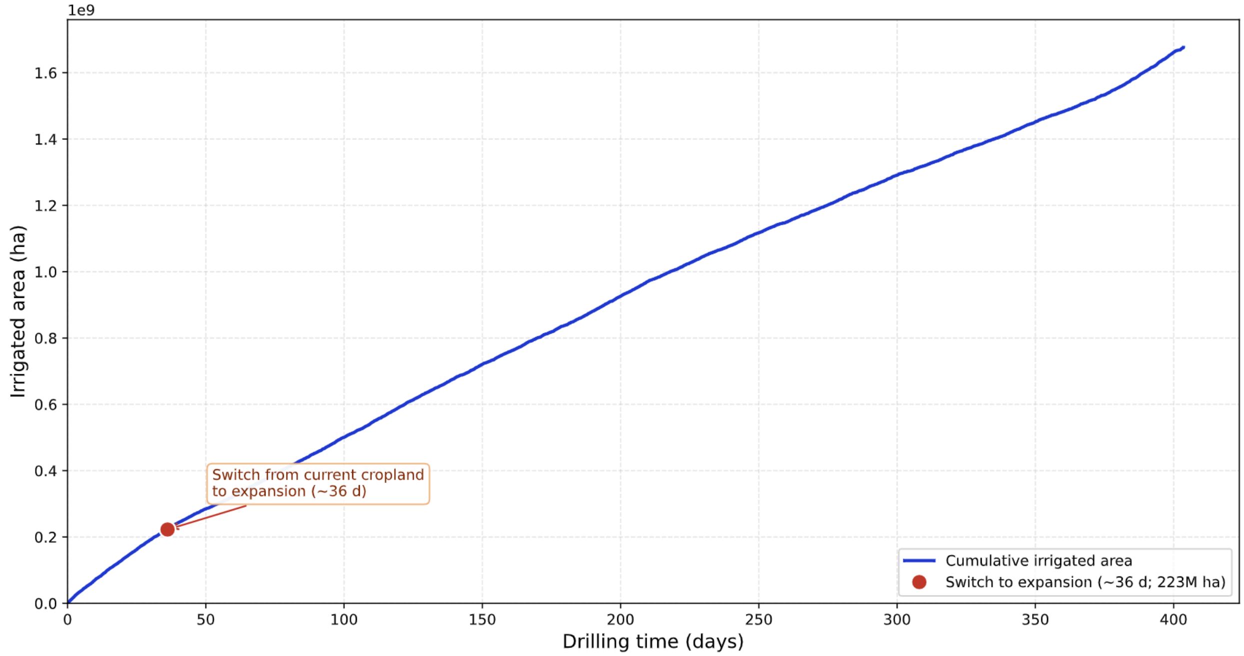

Figure C1. Progress of irrigated area versus drilling time for current and expanded cropland with unbounded food cost.

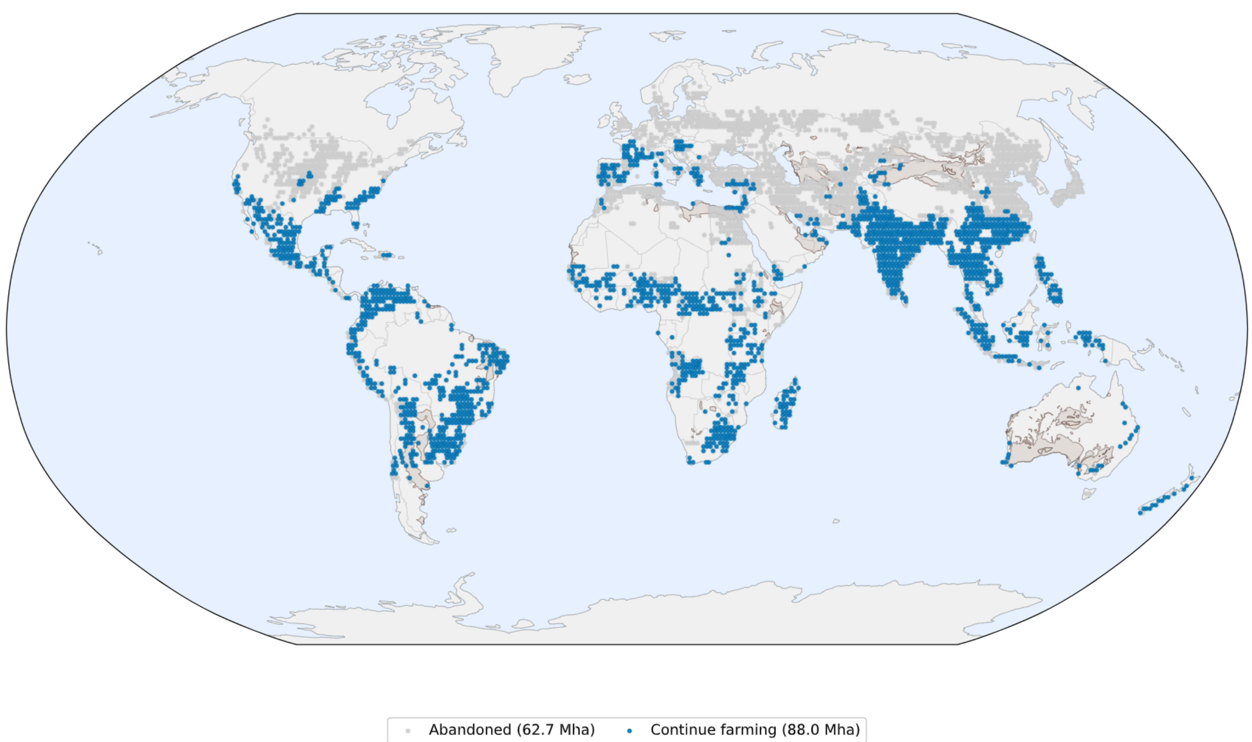

Figure C2. Existing irrigated cropland decisions under the 150-Tg ASRS case for analysis years 2–8, with investment allowed on both current cropland and expansion land (expansion not shown), at a total investment budget of $8.935 trillion.

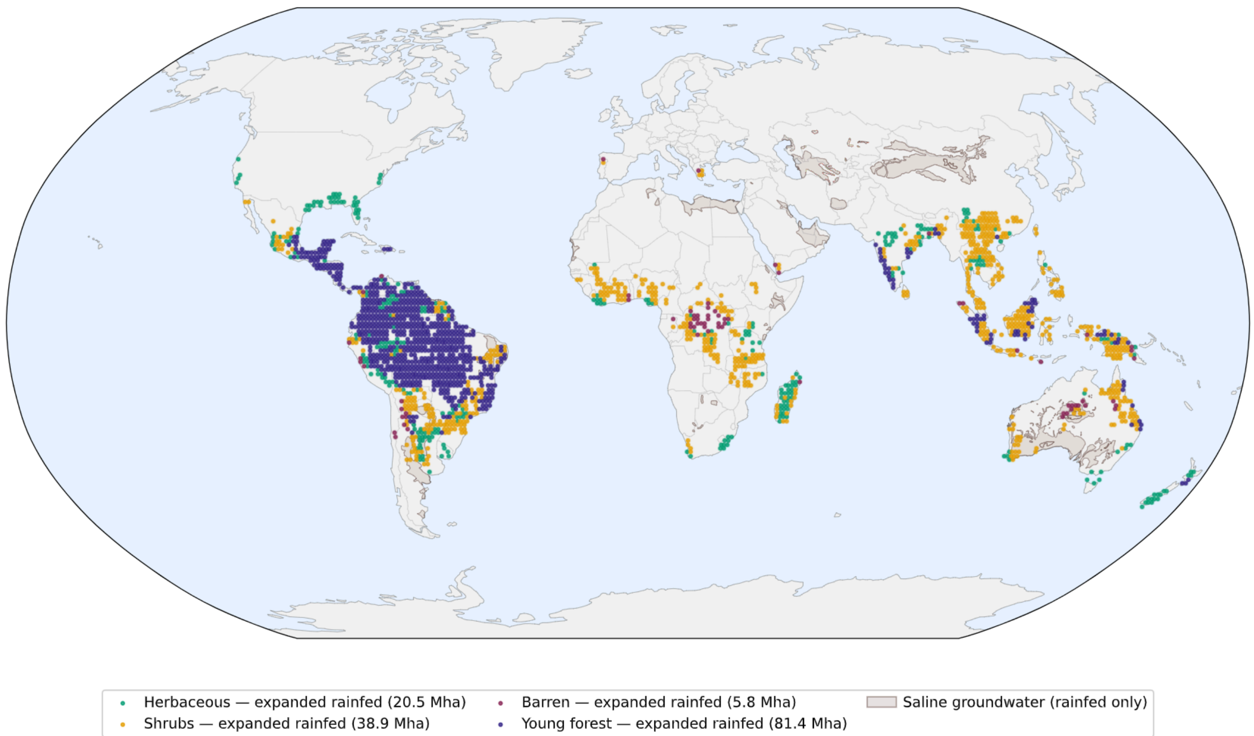

Figure C3. Rainfed expansion onto non-cropland in the optimal allocation. Each grid cell and land-cover class is optimised separately. The map shows rainfed expansion (R) only; existing cropland is omitted. Where multiple expansion classes occur in one cell, one marker shows the class with the largest expansion area. Legend values indicate the number of hectares by class. Gray shading indicates saline-groundwater zones, where only rainfed cultivation is allowed.

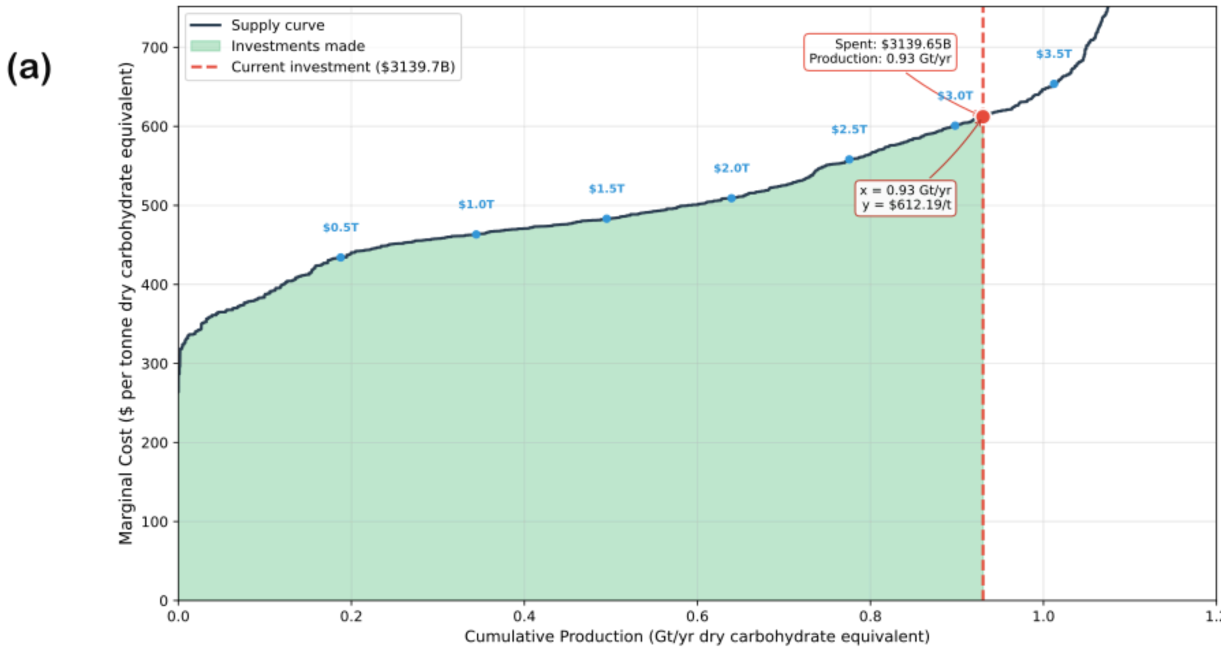

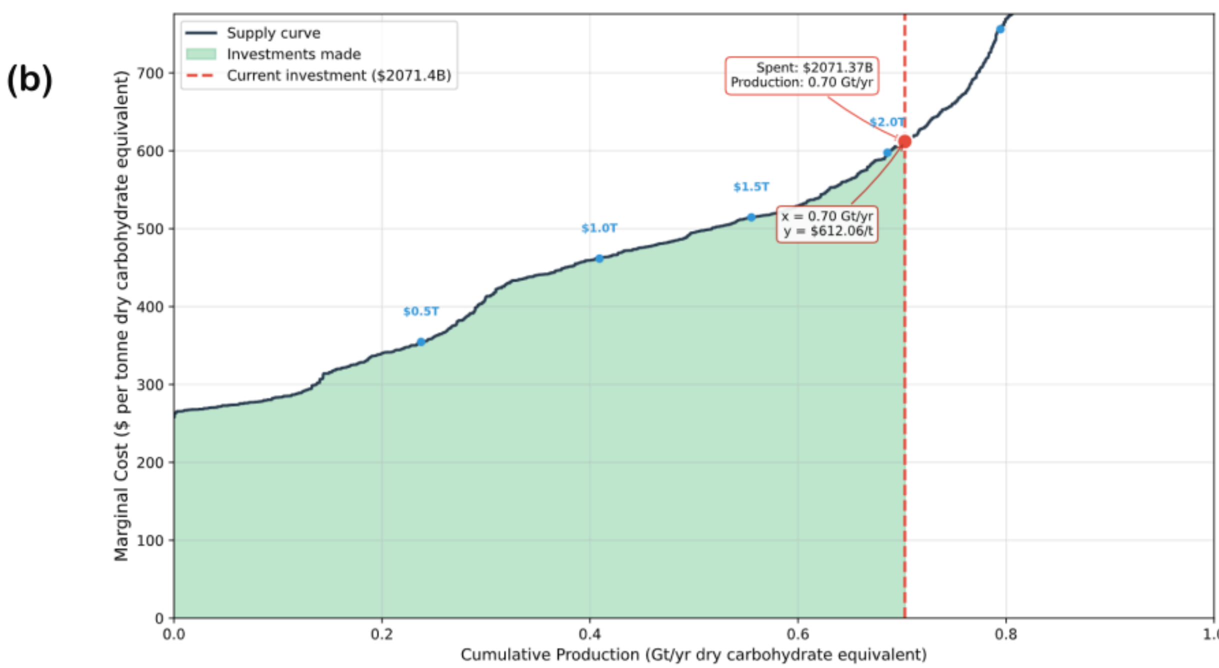

Figure C4. Per-country supply curves for (a) Australia (b) Brazil under the 150-Tg ASRS case (analysis years 2–8) for different investment budgets.

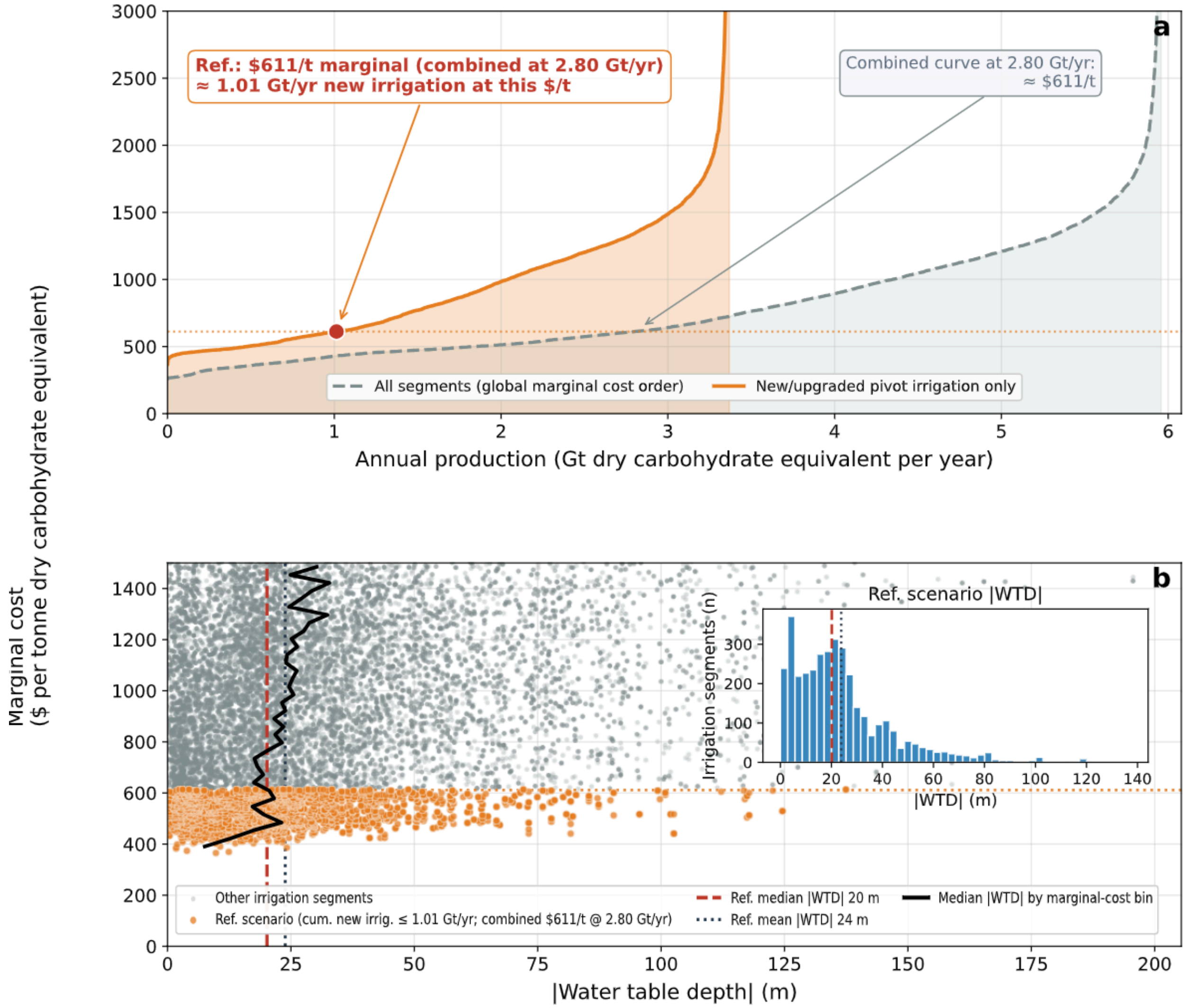

Figure C5. (a) Full cost frontier of all investment segments in ascending marginal-cost order, and the irrigation-only subsequence along that order. (b) Water-table depth when each (cell × land-cover) first reaches I*/RI* in that order; Dashed line indicates the median staples reference on the combined curve in panel (a).